Use Authorization

In presenting this thesis in partial fulfillment of the requirements for an advanced degree at Idaho State University, I agree that the Library shall make it freely available for inspection. I further state that permission to download and/or print my thesis for scholarly purposes may be granted by the Dean of the Graduate School, Dean of my academic division, or by the University Librarian. It is understood that any copying or publication of this thesis for financial gain shall not be allowed without my written permission.

Signature Jacob McMillan

Date 9-3-14

THERMAL ROCKET NUCLEAR DESIGN EVALUATION AND MODIFICATION USING MCNP

By

Jacob Bryan McCallum-Clark

A thesis

Submitted in partial fulfillment

of the requirements for the degree of

Master of Science in the Department of Nuclear Engineering and Health Physics

Idaho State University

October 2013

To the graduate faculty:

The members of the committee appointed to examine the thesis of Jacob McCallum-Clark find it satisfactory and recommend that it be accepted.

Jay J. Kunze 1/30/2014

Dr. Jay Kunze
Major Advisor

G. R. Imel 1/30/14

Dr. George Imel
Committee Member

H. Mousavinezhad 1-30-2014

Dr. Hossein Mousavinezhad
Committee Member

ACKNOWLEDGEMENTS

The author would like to acknowledge Dr. Jay Kunze for his input and expertise in the design process and completion of this project. Additional thanks is given the ISU nuclear engineering department professors and faculty for their knowledge and teachings that made this project possible.

VITA

Jacob Bryan McCallum-Clark was born in Seattle, WA in 1989, and was raised in the Seattle area until the age of 17 when he moved to Wenatchee, WA. He graduated from Wenatchee High School in 2007 and immediately moved to Spokane to attend Whitworth University. In 2011, Jacob graduated with a B.S. in Physical Chemistry and a B.A. in Applied Physics. Three months later, he moved to Pocatello, ID to attend graduate school at Idaho State University where he received a Master of Science in Nuclear Engineering upon the completion of this thesis in October, 2013.

TABLE OF CONTENTS

LIST OF FIGURES

LIST OF TABLES

SYMBOLS AND TERMINOLOGY

NTR -	Nuclear Thermal Rocket
I_{sp} -	Specific Impulse (Thrust/Propellant Flow Rate)
M -	Molar Mass (g/mol)
Be -	Beryllium
UO_2 -	Uranium Dioxide
W -	Tungsten
Re -	Rhenium
Ta -	Tantalum
B_4C -	Boron Carbide
CDs -	Control Drums
MCNP -	Monte Carlo Neutron and Photon (Transport Code)
RHP -	Right Hexagonal Prism
k_{eff} -	Effective Multiplication Factor
k_{excess} -	Multiplication Factor Fraction Above 1.0000
MeV -	Million Electron-Volts

ABSTRACT

The original idea for the solid core nuclear rocket was initially proposed back in the late 1950s. The General Electric (GE) 710 nuclear reactor was one of the initial designs employing this concept, developed under joint sponsorship by the Air Force and NASA. Utilizing stored liquid hydrogen as propellant and coolant for the reactor, specific impulses approximately twice that of a chemical rocket could be obtained. This high specific impulse significantly decreased the amount of fuel necessary for a round-trip Mars mission. The objective for this study was to examine, using the MCNP neutron transport program, various design parameters for the reactor creating thrust for the nuclear thermal rocket (NTR). Major focusses include: maintaining adequate excess reactivity, obtaining an appropriate amount of control, flattening the radial power across the reactor, evaluating the nuclear effects of different materials, and a brief analysis of a manned mission to Mars and back to Earth. A final design proposal is provided as a result of various perturbations made on the reactor dimensions. This final design provides a 10% range in k_{eff} from 0.948 with the control drums rotated toward the core, to 1.047 with the control drums rotated away from the core. Evidence is provided ensuring that this is more than enough excess reactivity to account for reactor operating parameter changes and burn-up on the entire trip.

1.0. BACKGROUND

1.1. Nuclear Power for Rockets

Utilizing nuclear fission as a means of rocket propulsion is a concept that has been around for more than 50 years. The original idea for the solid core nuclear rocket was initially proposed back in the late 1950s (Koenig, 1968). Unfortunately science was limited by technology of that time. As it is now 2013, the feasibility of utilizing thermal nuclear propulsion to be used for space exploration has been brought to the forefront, with the ultimate purpose to land a human on Mars and bring them back to Earth where the flight time in each direction is approximately 180 days (Borowski, 1993).

The reason for the re-hashing of ideas is predicated on the potential for a launch from Earth's orbit. Being that nuclear fission is the means of thermal propulsion, a launch from Earth atmosphere posed an immediate threat. As such, launching from Earth's orbit, such as the International Space Station, become viable options for turning a once innovative idea into a reality.

The desire to create the fastest propellant exit speed for a given flow rate is one of the primary goals in advancing rocket propulsion technology. The current chemical system approach is burning hydrogen and oxygen in order to provide thrust for the rocket. Specific Impulse (I_{sp}) "represents the force with respect to the amount of propellant used per unit time (Northwestern, 2009)." Essentially, the amount of energy that each atom of the propellant obtains in the thrust chamber of the rocket is directly proportional to the specific impulse. The reason that a solid core nuclear rocket is being considered is for the purpose of increasing the specific impulse substantially above that of the chemical rocket. An increase in temperature and a decrease in the molecular weight of the propellant provide a larger specific impulse being that I_{sp} is proportional to the square root of temperature and inversely proportional to the square root of the molar mass (m) of the propellant (Eq. 1.).

(Eq. 1.) $$I_{sp} = 9.797\sqrt{\left(\frac{k}{k-1}\right)\left(\frac{T_c}{m}\right)\left[1-\left(\frac{P_e}{P_c}\right)^{\frac{k-1}{k}}\right]}$$ (in seconds) where k is ratio of specific heats of hydrogen (1.40 at room temperature and 1.36 at 1000^{o}C)

T_c is the nozzle exhaust temperature

P_e/P_c is the ratio of the nozzle exhaust pressure divided by the discharge reactor pressure

The current chemical process burns oxygen and hydrogen where M=18g/mol. Burning simply H_2 provides M=2g/mol. In fact, the solid-core thermal nuclear rocket is theorized to have a specific impulse (~850s) that is approximately twice that of the current rocket chemical propellant (~350s) (Karlheinz, 1970). Other theoretical models have suggested even higher specific impulses, such as the gas-core nuclear rocket or ion propulsion. However, such concepts are not nearly as well developed as the solid-core reactor.

1.2. Reactor Concept

The General Electric (GE) 710 nuclear reactor was designed to use highly enriched uranium as the primary fuel source. The heat created from fission of the U-235 will be transferred to hydrogen which is used as both coolant and propellant. Increasing the thrust to weight ratio is the ultimate goal for a deep space mission. The tiny molar mass of hydrogen, coupled with the extreme temperatures in the core will provide a high specific impulse and thrust for the rocket. The idea is to store the hydrogen in its liquid state (less than 20K [Sigma-Aldrich, 2013]), and releasing it at a rate determined by the desired

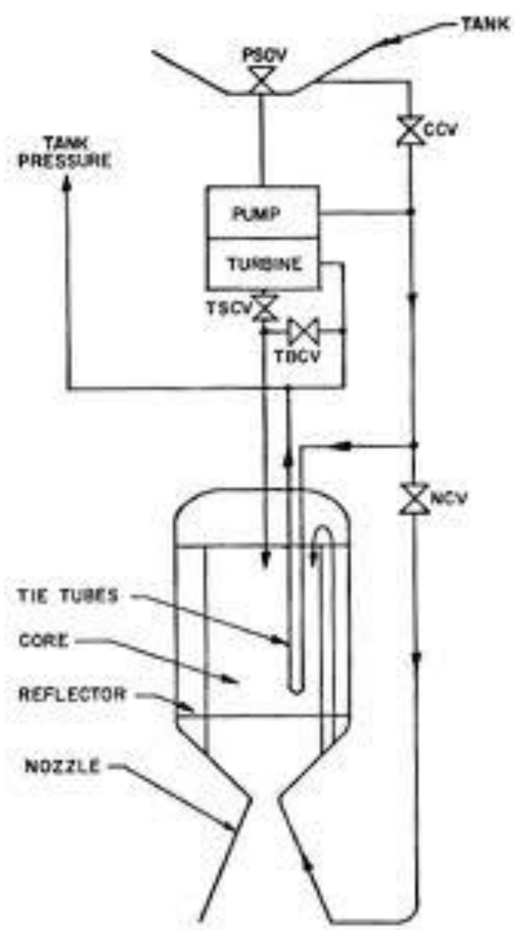

Fig. 1.1. Schematic for nuclear thermal rocket (Zandbergen, 2013)

thrust for the rocket. The hydrogen will then pass through a matrix of axial channels in the reflector before passing through another matrix of smaller, more numerous axial channels in the core, such that the total flow area of the hydrogen channels through the core and reflector are approximately the same. These larger reflector channels allow for less heat loss due to friction than the smaller ones, which is important because the primary heating of the molecules will not be in the reflector. Hydrogen will then be released through the nozzle providing thrust toward the front of the rocket, Figure 1.1.

2.0. PROPOSED REACTOR MODEL

The reactor should be a similar (yet modified by this thesis) version of the GE 710 reactor. As mentioned above, hydrogen serves to function as both propellant and coolant for the reactor located inside the thrust chamber. The reactor was designed to maximize heat transfer to the hydrogen in order to increase the thrust of the rocket as much as possible. Large coolant channels in the beryllium (Be) reflector allow for adequate hydrogen flow while limiting losses due to friction. Control drums (CDs) are used to provide appropriate change in reactivity in order to maintain criticality throughout the mission, yet allowing for the reactor to quickly shut itself down. The control drums will rotate such that a wedge of boron-carbide (B_4C) poison on each drum can be positioned in order to achieve this goal. The voids in the core matrix constitute 30% by volume of the entire core. The other 70% consists of fuel coupled with a combination of other materials whose effectiveness is examined throughout this thesis.

2.1. Core Materials Allocation

The reactor core was designed such that there is a hybrid of materials to provide both structural integrity and be used as the fuel in the core. Microsphere Uranium Dioxide (UO_2) fuel kernels will be placed inside either a tungsten-rhenium (W-Re) or tungsten-tantalum (W-Ta) hybrid material. W, Re, and Ta all have melting points greater than that of the UO_2 fuel kernels (Sigma-Aldrich, 2013), causing the UO_2 to be the limiting factor in the maximum allowable temperature inside the thrust chamber. These melting points are shown in table 2.1.

Table. 2.1. Melting points of various materials found in core (Sigma-Aldrich, 2013)

Material	Melting Point (K)
W:	3683
Re:	3453
Ta:	3269
UO_2:	3140

Certain volume and weight fractions of each of these materials were needed in order to provide proper balance between structural integrity and the amount of fuel necessary to allow the reactor to go critical. Figure 2.1 displays the material breakdown inside the core. Out of the 70% solid matter making up the core, 50% by volume is UO_2 fuel kernels, while the other 50% is the W-Re or W-Ta structure. For the purpose of this thesis, the W-Re-UO_2 or W-Ta-UO_2 was lumped into a single hybrid material in order for geometrical simplicity in utilizing MCNP to model this reactor. Of the 50% W-Re or W-Ta, 75% by weight was designated as the W, while the remaining 25% is either Re or Ta. The UO_2 enrichment was varied as a result of an attempt to flatten the power radially across the core. This will be addressed later in this thesis. The material breakdown by each isotope's normalized weight percent can be observed in Table 2.2. The values examined in the table are not necessarily the enrichments of each isotope, rather they are based on enrichment and material percentages defined above. The extended calculations can be seen in Appendix A.

Table 2.2. MCNP input deck isotopic abundance by weight fraction to define solid materials inside the core; Uranium values vary based on enrichment; Left- W-Re-UO_2 hybrid, 91% enriched U-235; Right- W-Ta-UO_2 hybrid, 89% enriched U-235; Reference Appendix A for detailed calculation

Isotope	Weight Fraction
Re-185	0.06367
Re-187	0.10772
W-182	0.12350
W-183	0.06706
W-184	0.14493
W-186	0.13541
U-235	0.28649
U-238	0.02838
O-16	0.04284
	1.00000

Isotope	Weight Fraction
Ta-183	0.14103
W-182	0.12803
W-183	0.06951
W-184	0.15024
W-186	0.14037
U-235	0.29046
U-238	0.03595
O-16	0.04441
	1.00000

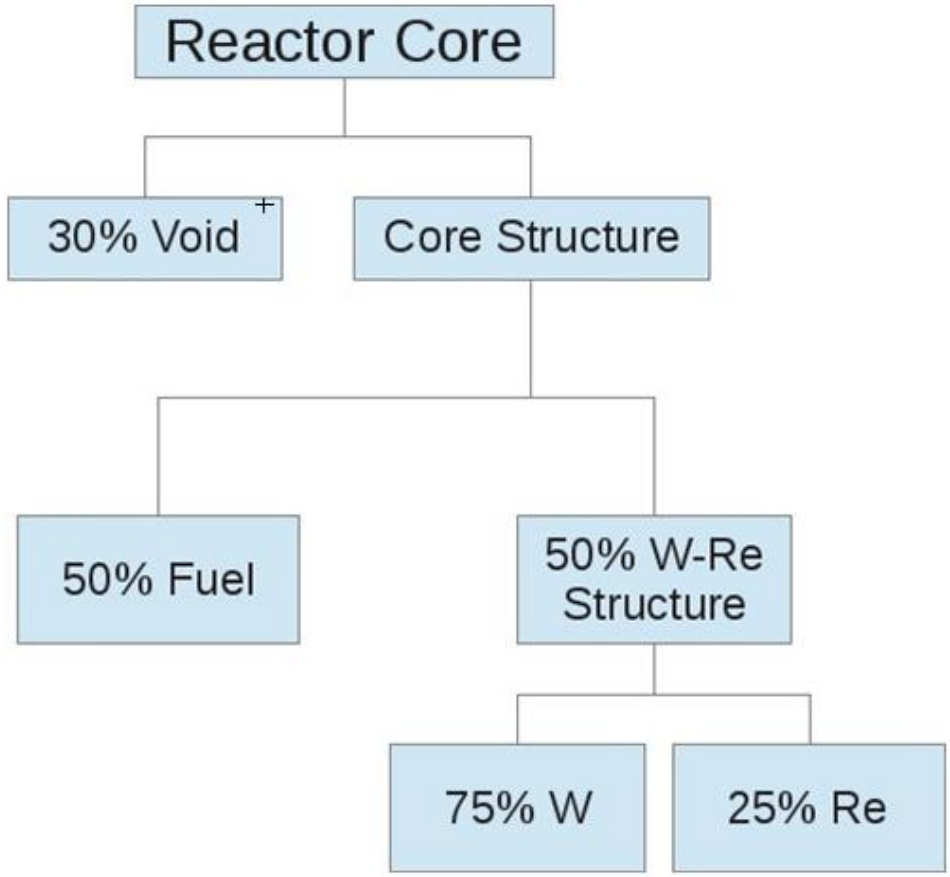

Fig. 2.1. Materials breakdown of the core of the reactor
* Contains $8.9*10^{-5}$ g/cm^3 H_2 gas at 3073K

2.2. Reflector Design

The Be reflector design surrounding the core initially had a 15cm thick shell surrounding the core periphery and a six CDs. The CDs should each contain a thin 90^o wedge of Boron Carbide (B_4C) that can be rotated to either increase or decrease reactivity based on the angle of each drum. This thesis will examine the range in k_{eff} values that result from different geometries constructed for the purpose of maximizing the range between the CDs rotated in versus CDs rotated out.

3.0. INITIAL REACTOR DESIGN USING MCNP

3.1. Fuel Element Construction

As mentioned previously, each assembly must be created such that 30% by volume is hydrogen coolant channels and 70% is the solid core material. Utilizing hexagonal lattices in MCNP provided the most efficient way of constructing an assembly. A 1.5mm diameter cylindrical hydrogen channel was the baseline dimension to constructing the rest of the core. Knowing that this must be 30% of a unit cell, a right hexagonal prism (RHP) was placed around the outside and filled with the W-Re-UO_2 material such that it made up 70% of the RHP and the cylinder made up 30%. These unit cells were then placed into a hexagonal lattice, which made up a pre-calculated larger RHP that filled a full assembly (Fig. 3.1.)

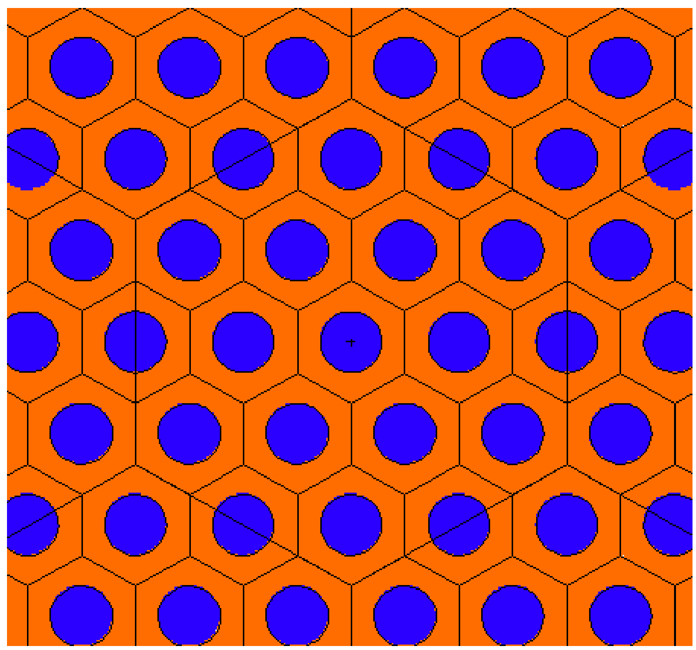

Fig. 3.1. Lattice of fuel and coolant channel cells that make up an assembly to be duplicated in the core

3.2. Reactor System Design

The first reactor design was an attempt to create a super-critical to sub-critical range in k_{eff} providing the cases of the control drums (CDs) rotated in versus rotated out. There was also information provided from a previous thesis that radial enrichment variations will be necessary in obtaining a flat radial power distribution across the core. The initial core construction and baseline geometry information can be observed in Figure 3.2. Variations on the geometric parameters provide an idea of the different possibilities for the construction of the core. The following section will provide changes in various parameters of the reactor construction and the effect that they had on k_{eff}.

Upon the creation of a single assembly, each one was then placed into a larger lattice which makes up the entire core. In order to obtain varying radial enrichment zones, different assemblies had to be made with modified materials that accounted for the change in enrichment. Each of the new assemblies were then individually placed into an approximately symmetrical pattern with the lower enriched uranium at the center and raising the enrichment travelling radially outward. The enrichment zones exist as 85%, 87%, 89%, 91%, and 93% enriched in U-235 respectively. Slight variations to the assemblies along the outer periphery were made, which will be addressed later on. These zones were created using the hexagonal lattice fully specified fill feature of MCNP.

The Be reflector was made in one section and translated six times around the core periphery. A single control drum was placed in each section with a 90^{o} B_4C wedge rotated toward and away from the core. The hydrogen channels were placed such that their total volume would approximately equal the volume of the channels inside the core. Each channel has a 5cm radius and was individually placed in the single reflector section. After being translated six times, the entire reflector obtained its shape thus providing the entire reactor structure (Fig. 3.2)

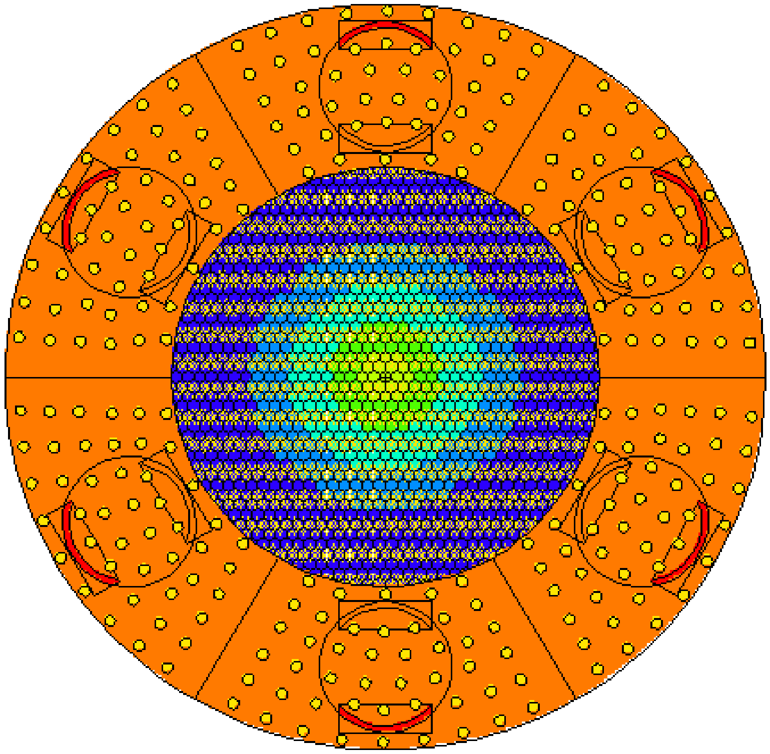

Fig. 3.2. W-Re-UO_2 design; 19.2cm radius core; 17cm reflector; 5 radial enrichment zones; six-6cm control drums; 90^o wedged 6mm thick B_4C; 70cm height; Above- CDs rotated away from core; Below- CDs rotated toward core

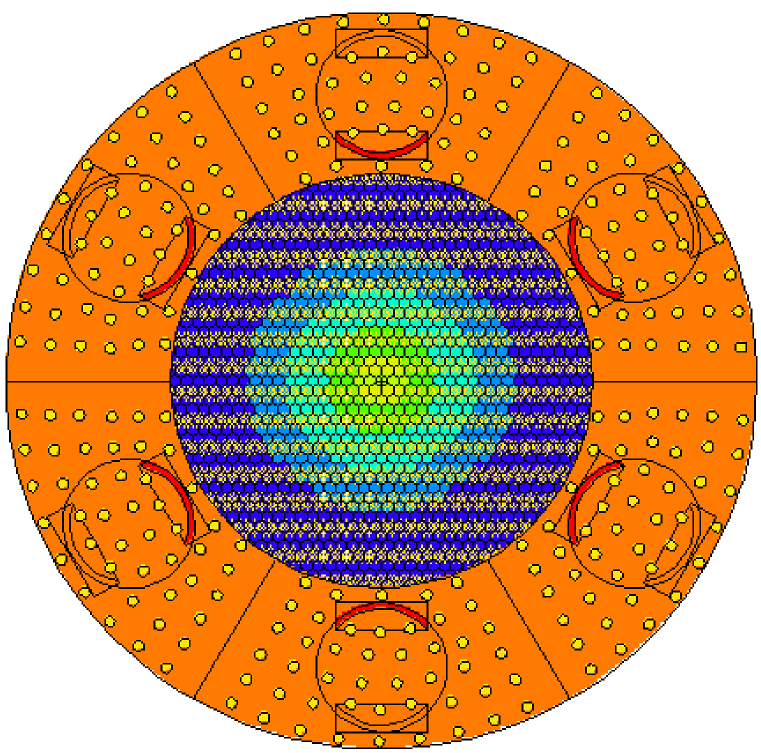

3.3. Varying Construction Parameters

The purpose for varying the different aspects of the core is to determine an adequate design that provides a large enough range in k_{eff}. The primary factor in obtaining a reactor with appropriate criticality is based on the radius of the reactor. Table 3.1 and figure 3.3 display the effects of changing the radius of the core and the corresponding values of k_{eff}. It appears based on the graph that as the radius increases, the range in values decreases noticeably. This can be attributed to the decrease in neutron importance as a result of moving further away from the center of the core. Each value was a tabulated average using 1000 initial particles averaged over 100 histories. A single history will follow each particle that was created during the last history through until a collision with another particle is made, whether it is a scattering or absorption. The initial goal was to achieve approximately 20% control over k_{eff} through turning the CDs toward the core (in) versus away from the core (out). The design parameters state that a 90^o section of B_4C located around the edge of each CD would be used in order to obtain this goal. The following tests were run on the original design for the reactor in order to determine how to maximize this amount of control.

Table 3.1. Varying radii of core; other variables kept constant

	6 CDs In:		***6 CDs Out:***		
Radius (cm)	keff	STDEV	keff	STDEV	Δ keff
15.0	0.88837	0.00189	0.96022	0.00192	0.07185
17.4	0.96228	0.00189	1.02036	0.00207	0.05808
19.2	1.01335	0.00199	1.06207	0.00189	0.04872

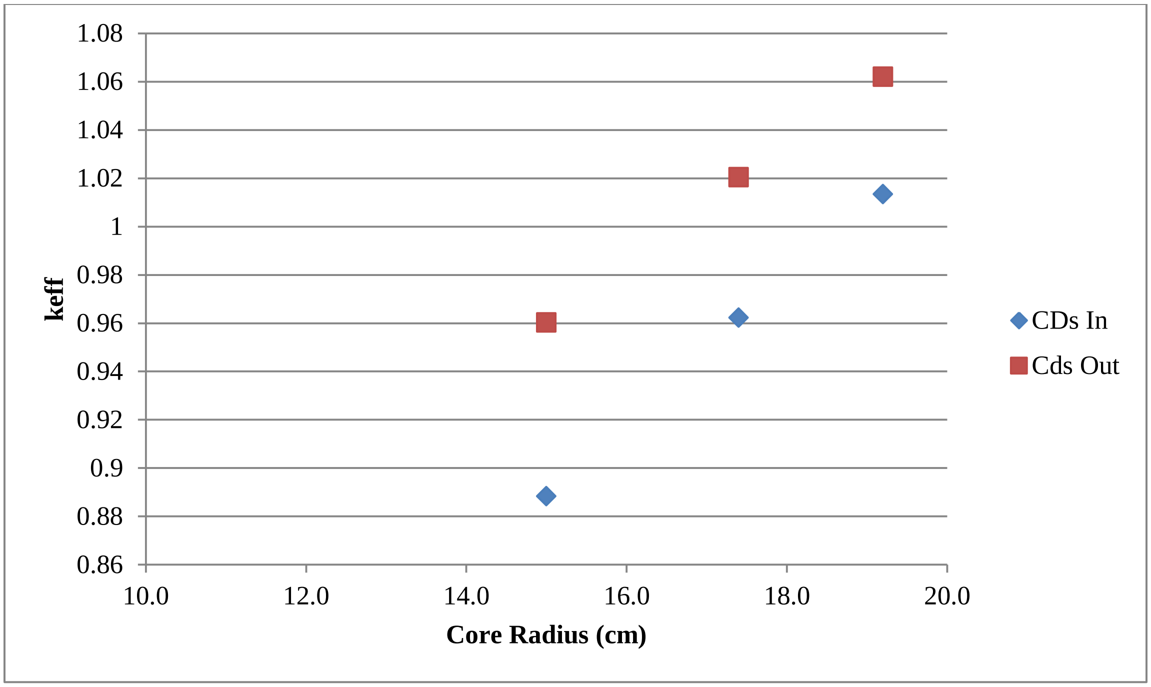

Fig. 3.3. Graph displaying varying radii of core for control drums rotated in (blue) and out (red)

It was also found that varying the reflector thickness provided a significant boost in the value of k_{eff}. However, it did not appear to have much effect on the range in values, maintaining approximately a 5% difference. It appeared that another method of expanding the range would have to be examined. The results from varying reflector thickness can be observed in table 3.2.

Table 3.2. Varying reflector thickness; other variables kept constant

	6 CDs In:		***6 CDs Out:***		
Refl. Thickness (cm)	keff	STDEV	keff	STDEV	Δ keff
15.0	0.99962	0.00197	1.04191	0.00229	0.04229
17.0	1.01335	0.00199	1.06207	0.00189	0.04872

Changing the thickness of the 90^o B_4C section on each control drum initially seemed that it would provide the amount of control needed by the reactor. However, after running a few tests, it became apparent that increasing the thickness past a certain point did not provide much difference in k_{eff}. In fact, the values converged to a point where increasing the B_4C thickness beyond about 6mm had almost no additional effect whatsoever. It was settled that 6mm thickness would provide as much control as needed without disrupting the geometry of the CDs too much. The results from the experiments run on k_{eff} can be seen in Table 3.3 and Figure 3.4.

Table 3.3. Vary B4C thickness; 15cm reflector; other variables kept constant

	6 CDs In:		***6 CDs Out:***		
B4C Thickness (mm)	keff	STDEV	keff	STDEV	Δ keff
2.0	1.0113	0.00197	1.04855	0.00175	0.03725
6.0	0.99962	0.00197	1.04191	0.00229	0.04229
10.0	0.99371	0.00206	1.04126	0.00201	0.04755

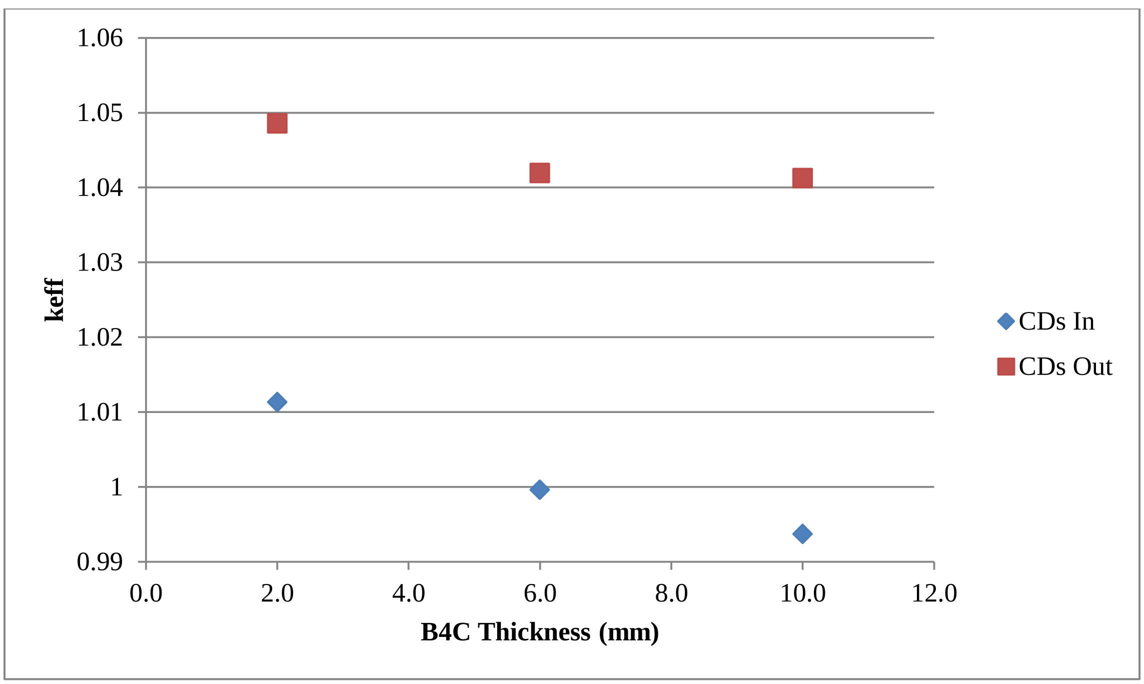

Fig. 3.4. Graph displaying varying Thicknesses of B4C for control drums rotated in (blue) and out (red)

The final aspect of manipulation on the six CD design was to change the height of the reactor, while maintaining a range in criticality that provided both super and sub-critical results. It seemed that a 70cm height should be the maximum height based on previous studies that had been done (Fischhaber, 2012). As such, decreasing the height in increments of 5cm was enough to show a pattern that changing the height provides. Once again, the results were disappointing in that there was not a major fluctuation in the range in k_{eff} values. Decreasing the height provided little fluctuation in Δk_{eff} until the height dropped below about 63cm. Table 3.4 and Figure 3.5 display the values and patterns obtained from the results. It was decided that the original specifications of 70cm height would be utilized for the final reactor design.

Table 3.4. Vary core height; 15cm refl; other variables kept constant

	6 CDs In:		***6 CDs Out:***		
Height (cm)	keff	STDEV	keff	STDEV	Δ keff
60.0	0.9748	0.00197	1.01320	0.00183	0.0384
65.0	0.98403	0.00182	1.02886	0.00202	0.04483
70.0	0.99962	0.00197	1.04191	0.00229	0.04229

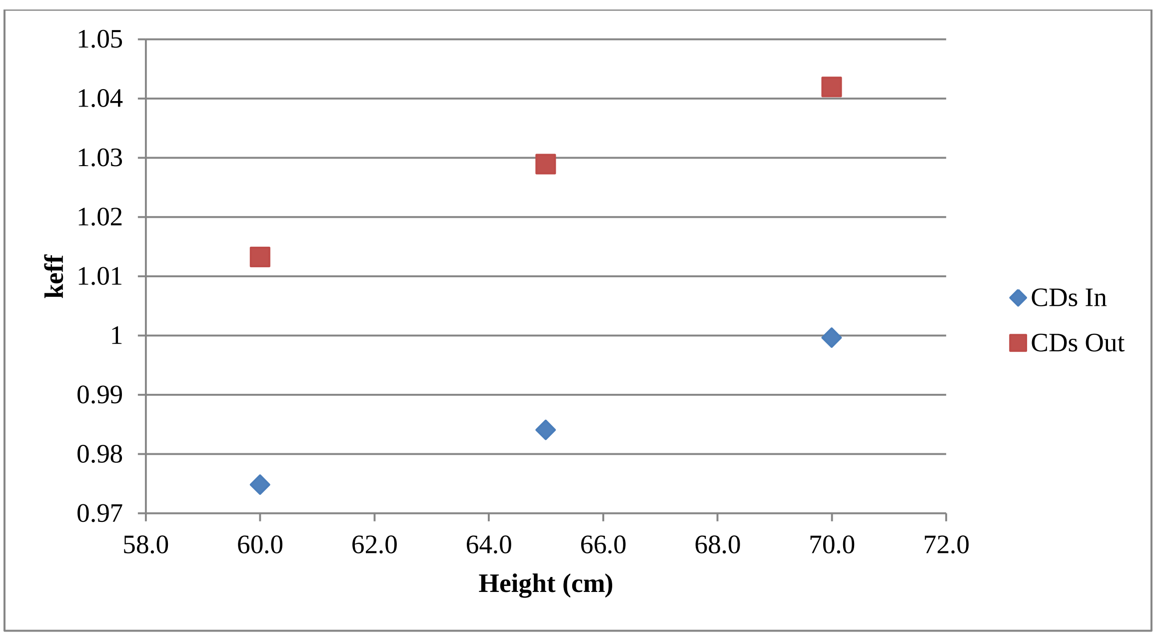

Fig. 3.5. Graph displaying varying heights of core for control drums rotated in (blue) and out (red)

In order to obtain a general understanding of what the neutron flux through the core and reflector looked like, an f4 mesh tally overlaid across the entire reactor. This particular mesh tally examines a cross section in the x-y plane, averaged over the entire height of the core, and tallies the neutron flux that passes through each section of the grid. The results are recorded in neutrons/cm^2. GnuPlot was the program that was utilized to create this particular graph (Fig. 3.6). It should be noted that this is a fast spectrum reactor with a negligent fraction of neutrons falling in the thermal range. The energy spectrum, divided into 19 energy groups, for this particular reactor, can be examined in figure 3.7.

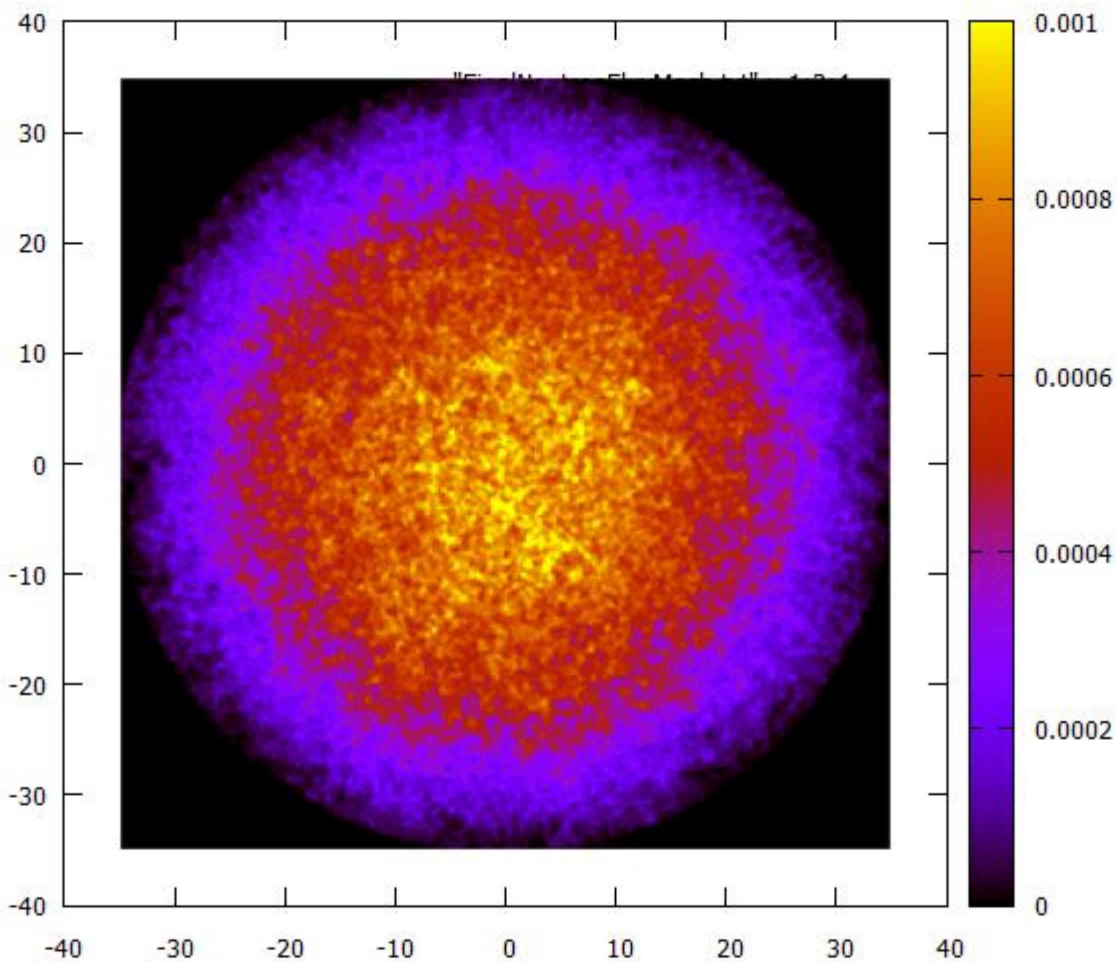

Fig. 3.5. Mesh tally in the center of the reactor in the x-y plane of the neutron flux (neutrons/cm^2) of the 6 drum configuration of the core and reflector; CDs out; 19.2cm core; 15cm refl; 6mm B_4C; 70cm height

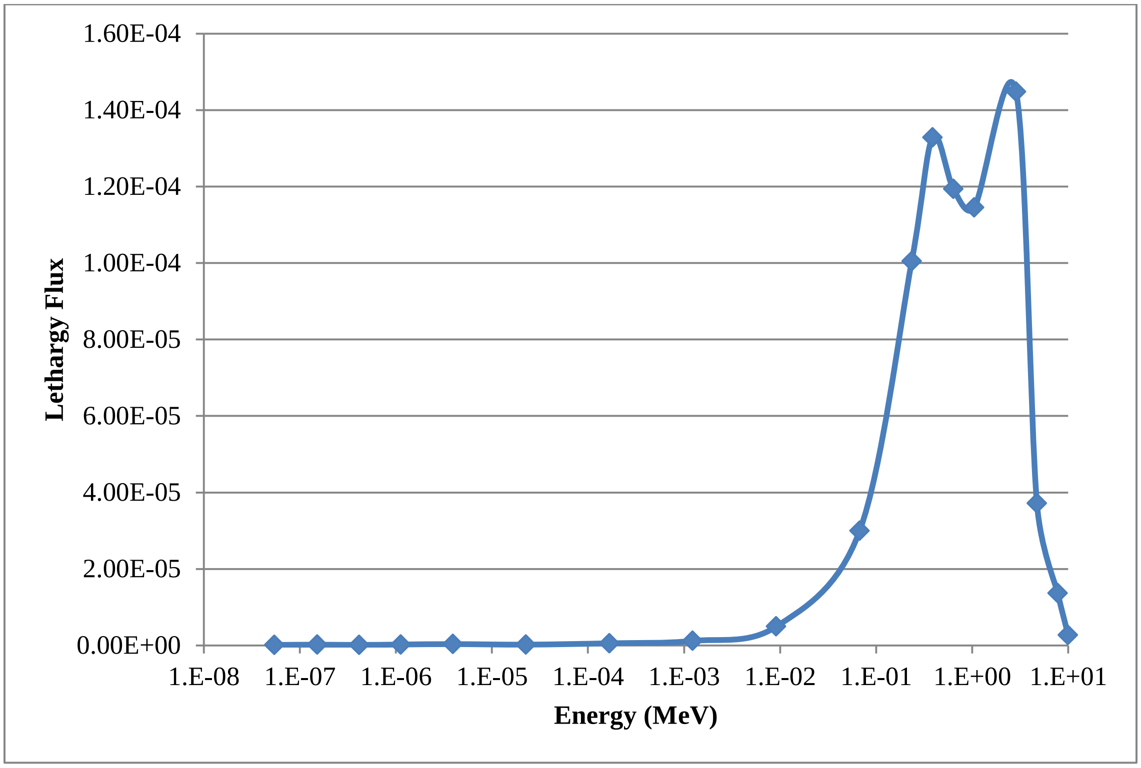

Fig. 3.6. Energy distribution lethargy plot displaying the neutron population divided into 19 energy groups

4.0. APPROACH TO FINAL REACTOR DESIGN

The largest range of k_{eff} values was only approximately a 6% change between the control drums rotated in versus rotated out; a change had to be made. It was determined that more control drums coupled with a larger radius and being moved as close to the core as possible would serve as a viable option for increasing the range of control. Much of the code had to be manipulated as a result including the rotational nature of the initial reflector section, the number and location of the hydrogen channels in the CDs and reflector, and the size and location of each drum. Through this process, more control was observed.

4.1. Changes from the Previous Design

For the most part, the shape of the core including the radial enrichment zones, were kept consistent with the initial design. The majority of the manipulation went into the design for the reflector and the CDs located inside. Previously, six-6cm CDs had been placed around the core. Being that not enough control could be manifested through slight tweaks in the design, something more drastic had to happen. It was determined that increasing the number of drums from six to nine along with moving them as close to the core as possible would provide the largest range in k_{eff}. Also, an increase in size from a 6cm radius up to 8cm should also increase the amount of control. This meant new rotational geometry and new placement in the reflector for CDs along with the hydrogen coolant channels. This new design and new baseline specifications can be observed in Figure 4.1.

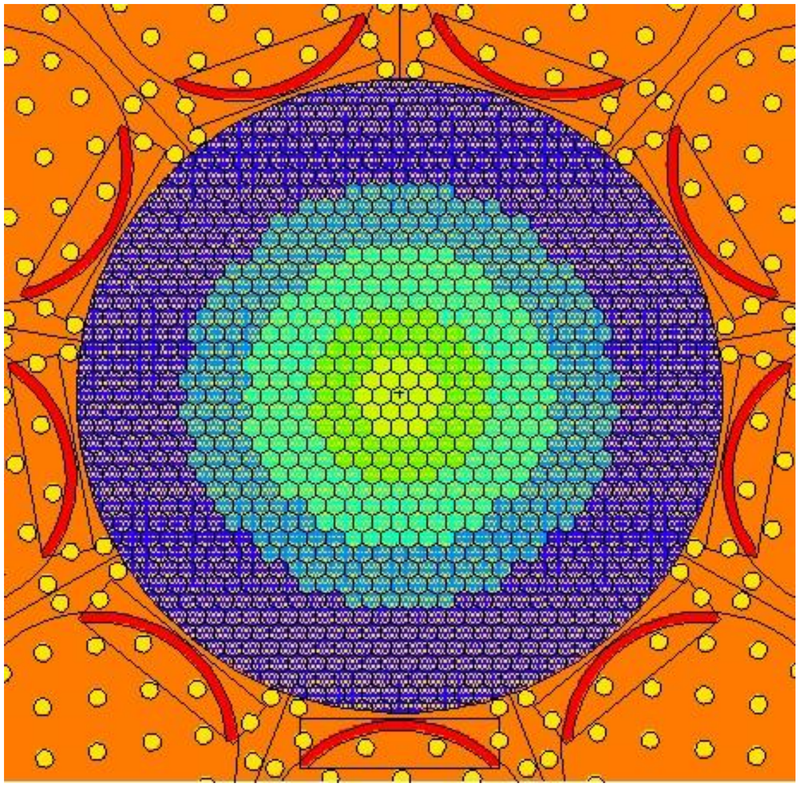

Fig. 4.1. New design for control drums in reflector in order to obtain maximum control. 18.2cm core; 17cm reflector; 6mm B_4C thickness; 70cm height; 5 radial enrichment zones; Nine-8cm control drums; Above-rotated toward core (close-up); Below-rotated away from core

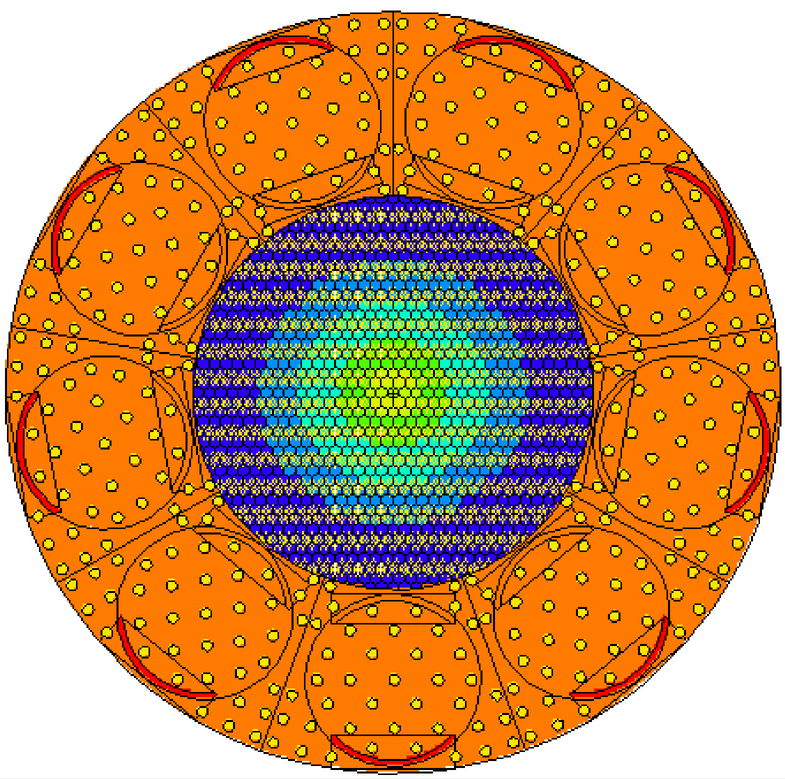

4.2. Examination of New Reactor Design

In order to obtain an understanding of the kind of control to be expected with the new design, a few different trials were run in MCNP. It was found that for the optimal range in k_{eff} values for W-Re-UO_2 design of the core, a 19.2cm radius would be the most appropriate option providing a reactivity swing of almost 10%. Table 4.1 provides the ranges in k_{eff} for the new design. Figure 4.2 displays the flux distribution radially through the core. This was done using the f4 mesh tally in a single dimension, unlike the x-y plane mesh tally that was done previously. With this improved control of the reactor, the next issue became flattening the power distribution across the entire core.

The following section will first examine then attempt to flatten this power distribution. The power distribution was determined using an f6 tally feature of MCNP which provides the MeV/g in each specified assembly (Fig. 4.3). By multiplying by the density of the material, the result becomes MeV/cm^3 which is a more standard result. The assemblies specified here were lattice elements moving out from the center in the x-direction. The outer-most data points that are substantially lower power level are assemblies that were placed at the edge of the reflector to ensure a drop in power after leaving the fissile assemblies. The tally is set up to measure energy from both neutrons and gamma rays in the core.

Table 4.1. W-Re-UO_2 core examining possible radii for final design of reactor; other variables kept constant

	9 CDs In:		***9 CDs Out:***		
Radius (cm)	keff	STDEV	keff	STDEV	Δ keff
18.2	0.93773	0.00184	1.03936	0.00212	0.10163
19.2	0.96372	0.00194	1.05965	0.00241	0.09593

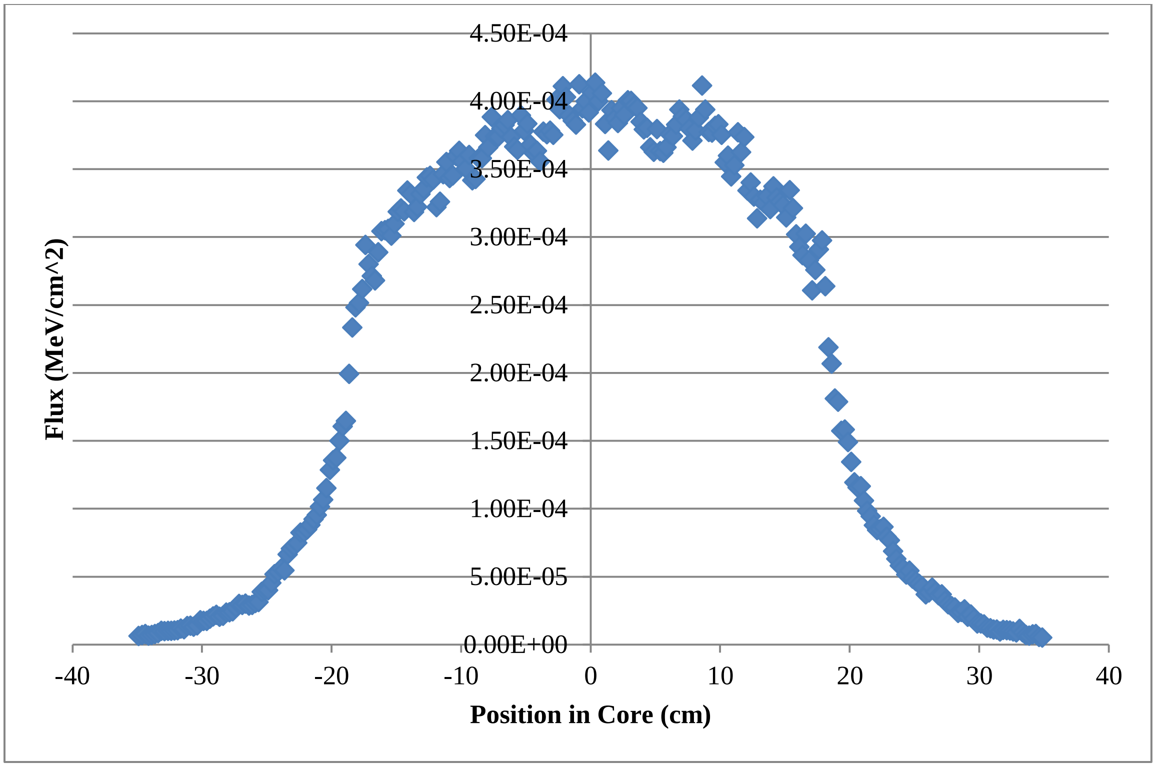

Fig. 4.2. Radial energy flux through W-Re-UO_2 core and reflector; 18.2cm radius; CDs *out*; 5 zone radial enrichment

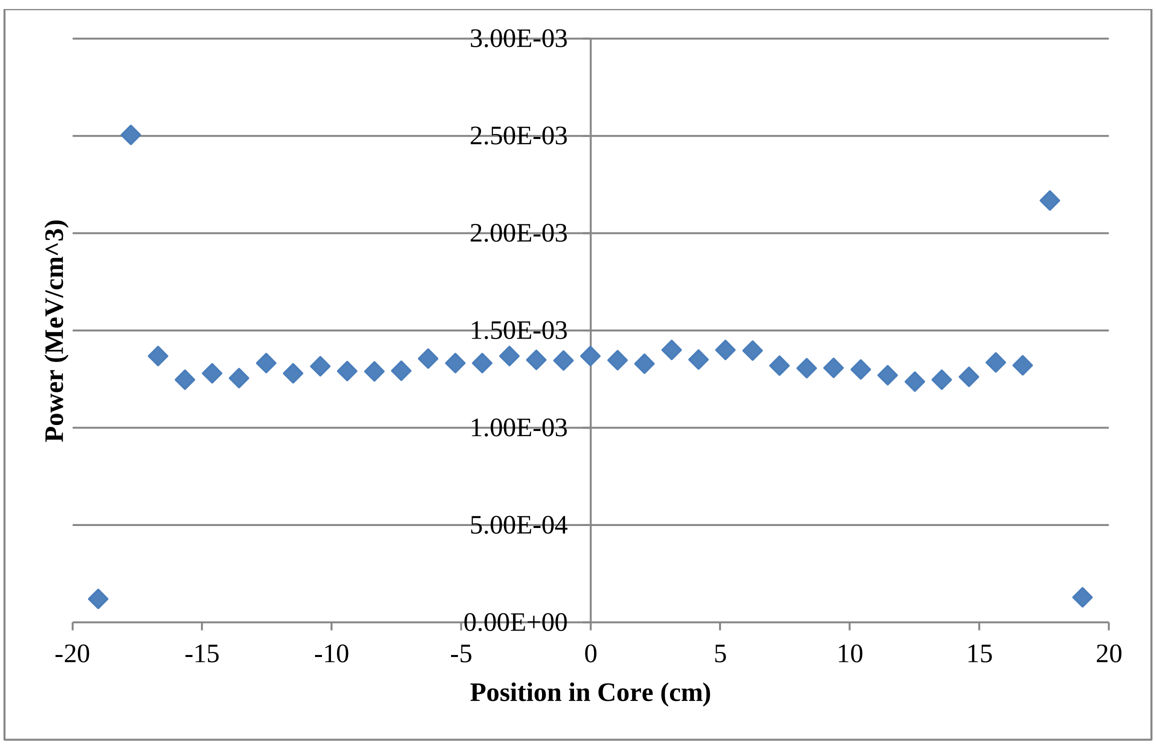

Fig. 4.3. Radial power distribution of W-Re-UO_2 core; 18.2cm radius; *CDs out*; 5 zone radial enrichment

Judging by the power distribution displayed in Figure 4.3, it was immediately apparent that the power was approximately the same throughout the majority of the core. The only region that appeared to not behave like the rest of the core was the outer-most assemblies. This power spike can be attributed to the proximity to the Be reflector. This issue had to be remedied somehow.

Initial estimates predicted that this power spike would be almost completely eradicated through simply turning the CDs toward the reactor. As such, the next test that was run was turning the CDs in and determining the resulting flux and power distributions (Fig. 4.4 and Fig. 4.5 respectively). These results proved to be approximately as expected. The loss of reactivity by replacing a piece of the Be reflector with a large absorption cross-section like B_4C appeared to have eliminated much of the power near the edge of the core, along with a substantial portion of reactivity.

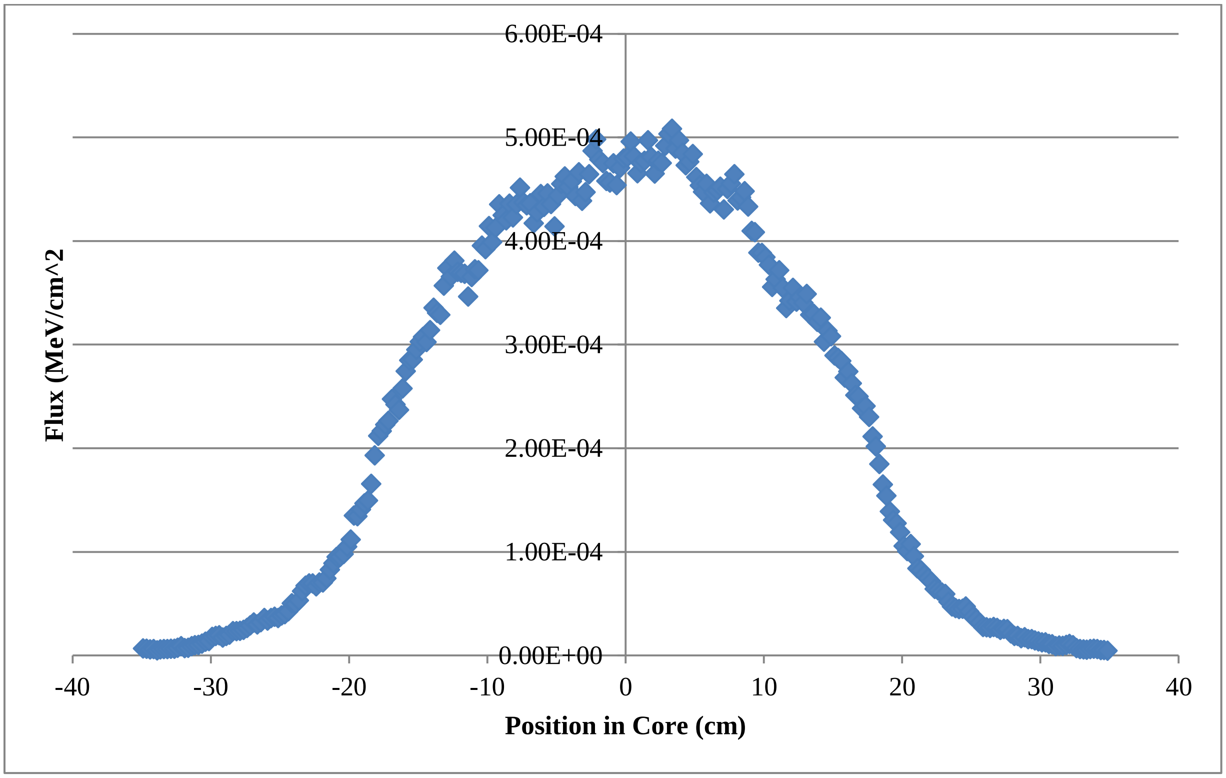

Fig. 4.4. Radial flux through W-Re-UO_2 core and reflector; 18.2cm radius; *CDs in*; 5 zone radial enrichment

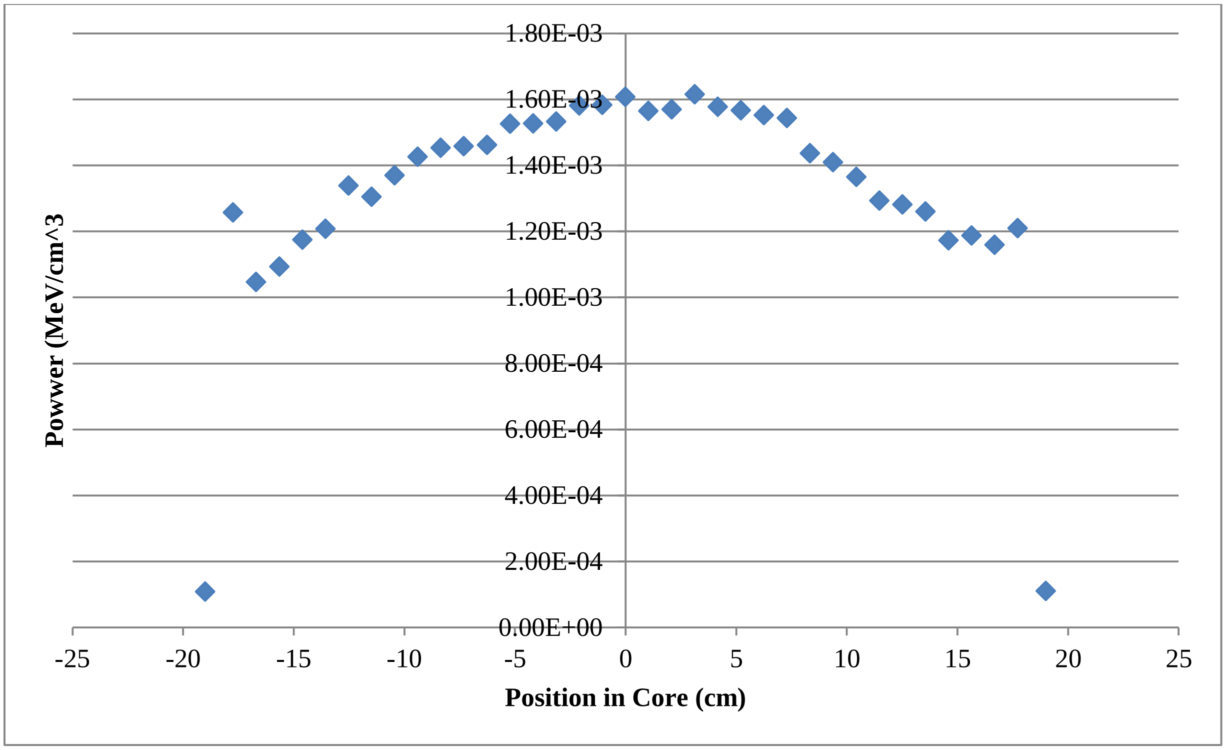

Fig. 4.5. Radial power distribution of W-Re-UO_2 core; 18.2cm radius; CDs *In*; 5 zone radial enrichment

4.3. The Switch to from W-Re-UO_2 to W-Ta-UO_2

Another option instead of utilizing Re for the core is to utilize Ta, which has a somewhat smaller absorption cross section. The two materials have very similar structural properties and high melting points capable of withstanding the extreme temperatures inside the reactor core. Ta does provide approximately a 2% bump in the amount of control available from 10% to approximately 12% by simply switching from Re to Ta (Table 4.2). The next step was to provide similar data as to the flux and power distributions in the reactor. Being that these two materials possess similar properties, it was believed that if the power of the W-Re-UO_2 hybrid could be flattened, so could the W-Ta-UO_2. Figure 4.6 and 4.7 show the flux and power distributions for the new material.

Table 4.2. Ranges in k_{eff} utilizing different materials; 18.2cm radius

	9 CDs In:		***9 CDs Out:***		
Core Solid Materials	keff	STDEV	keff	STDEV	Δ keff
W-Re-UO2	0.93773	0.00184	1.03936	0.00212	0.10163
W-Ta-UO2	0.94836	0.00193	1.06869	0.00212	0.12033

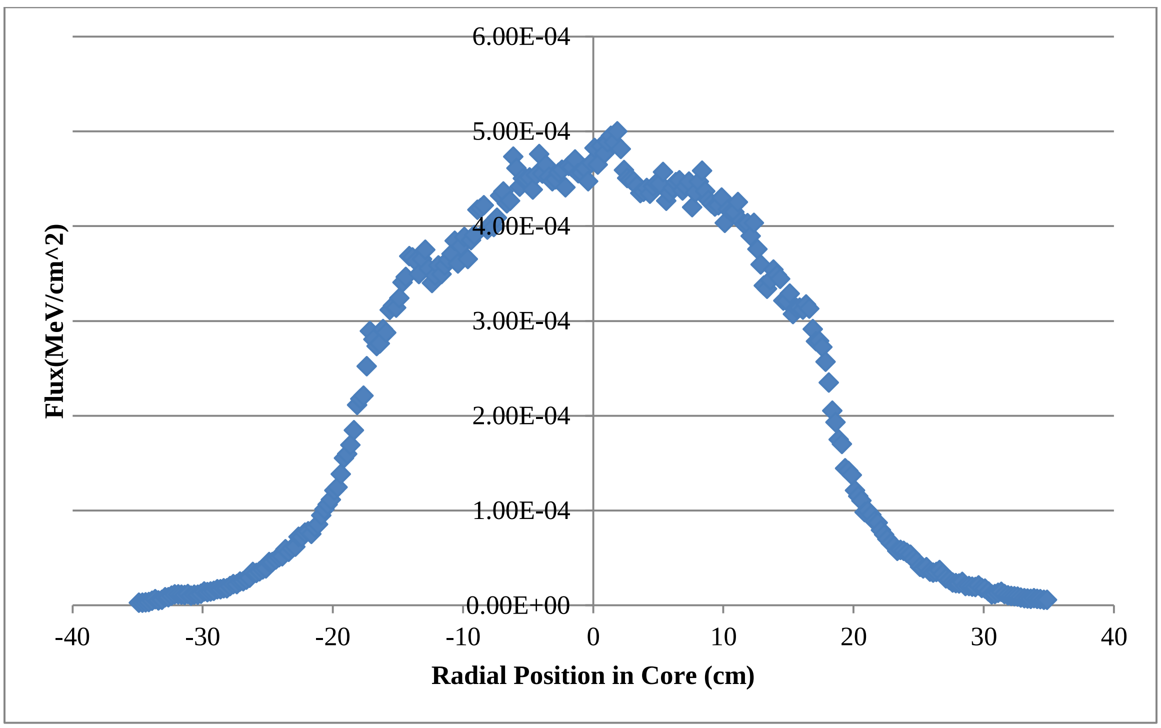

Fig. 4.6. Radial flux through W-Ta-UO_2 core and reflector; 18.2cm radius; CDs *out*; 5 zone radial enrichment

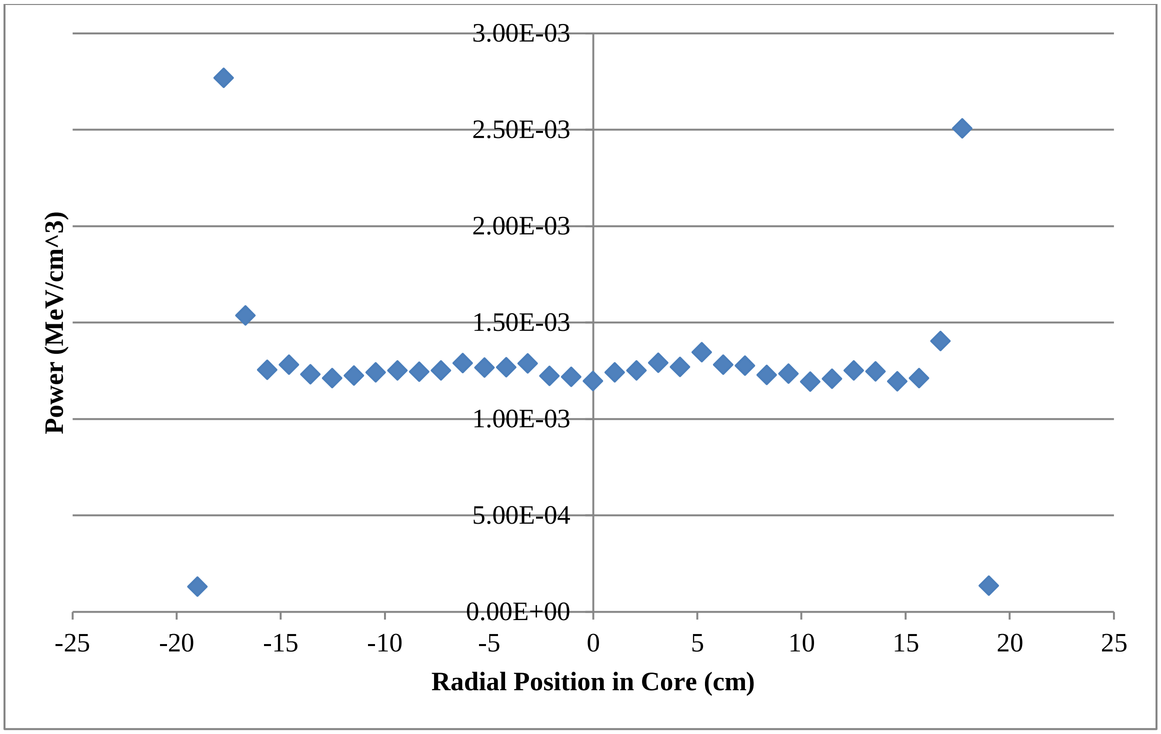

Fig. 4.7. Radial power distribution of W-Ta-UO_2 core; 18.2cm radius; CDs *out*; 5 zone radial enrichment

The power distribution appeared to have a very similar shape. The only major difference was that the power spike was slightly more drastic than that of the W-Re-UO_2 combination. Again, it seemed that something would have to be done in order to alleviate this power spike which is examined in the next section.

Judging by the results above, rotating the CDs in should provide very similar results to the power distribution of the W-Re-UO_2 core. The flux and power distributions can be observed in Figures 4.8 and 4.9 respectively. The results produce similar shapes using both materials. However, these distributions are very temporary in that the reactor quickly shuts itself down upon the loss of reactivity. This is simply an attempt to display how the reactor behaves upon shut down. Realistically, the CDs will be rotated somewhere between the in and out position in order to maintain criticality.

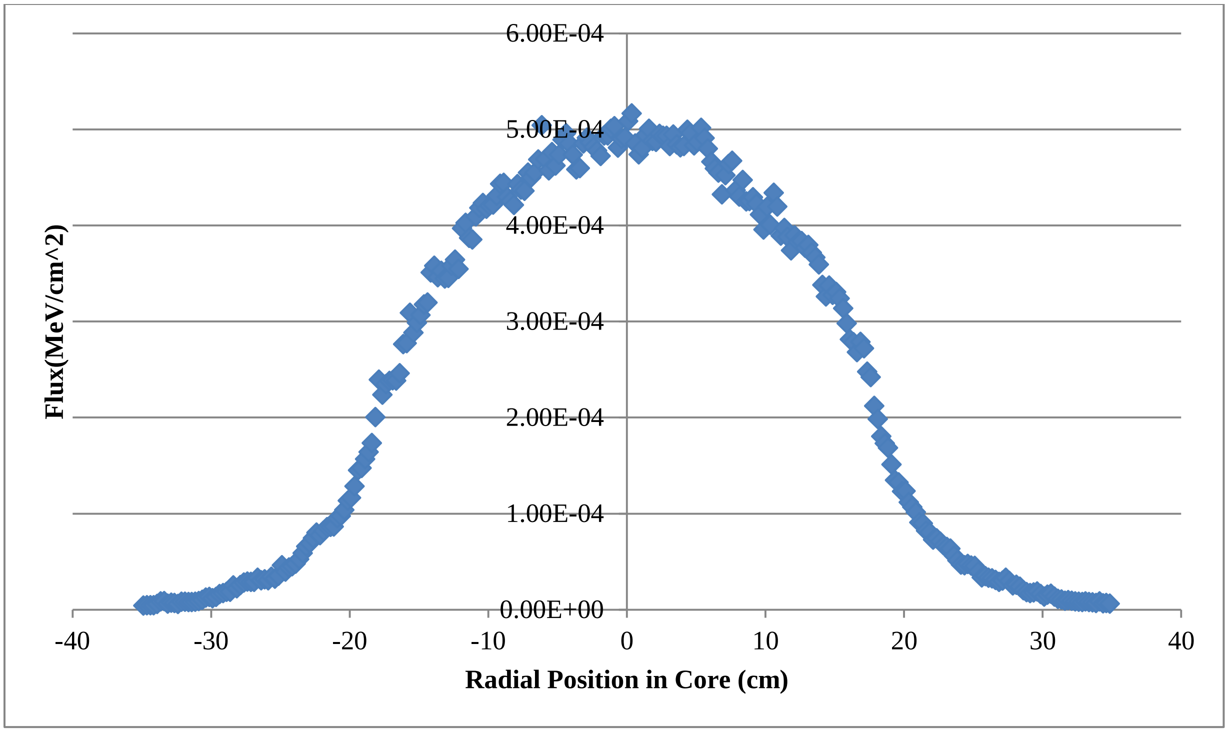

Fig. 4.8. Radial flux through W-Ta-UO_2 core and reflector; 18.2cm radius; CDs *in*; 5 zone radial enrichment

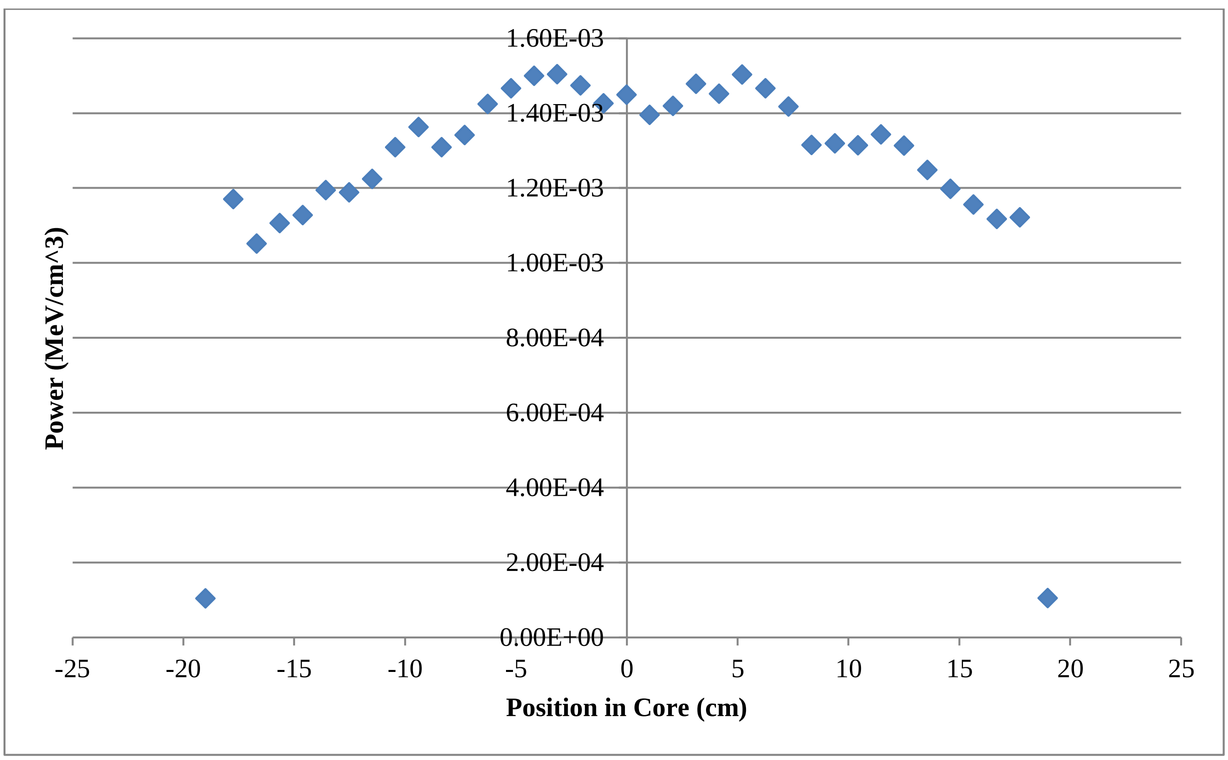

Fig. 4.9. Radial power distribution of W-Ta-UO_2 core; 18.2cm radius; CDs *in*; 5 zone radial enrichment

5.0. DECREASING THE POWER SPIKE NEAR THE REFLECTOR

Upon examining the preceding results, it became apparent that the varying radial enrichment zones accomplished their goal of flattening the neutron and gamma heating across the majority of the core of the reactor. However, the last two assemblies on the periphery had a large increase in power due to their proximity to the Be reflector when the reactor is running critical. When the control drums are rotated toward the core, this power spike is not readily observable. As a result, a series of steps were taken in attempt to alleviate the drastic heating increase to these assemblies while the control drums are rotated away from the core. The W-Ta-UO_2 hybrid was chosen to be tested instead of the W-Re-UO_2 primarily because the Ta material appeared to produce slightly higher ranges in k_{eff}, and very similar power distributions. It stands to reason that if Ta can be flattened, Re can be as well. Table 5.1 displays the values for k_{eff} for the following design modifications.

5.1. Initial Attempt

It was thought that increasing the coolant flow through the outer periphery might prove beneficial in decreasing the power to the region. As such, the radius of the axial voids in the outer assemblies was increased from a 1.5mm diameter to 2.122mm. This represents a switch from 30% void to 60% void and only 40% fuel matrix (Fig. 5.1). This design created a layer for increased power removal as to flatten the temperature profile around the entire outer edge of the core where the spike in power was previously observed.

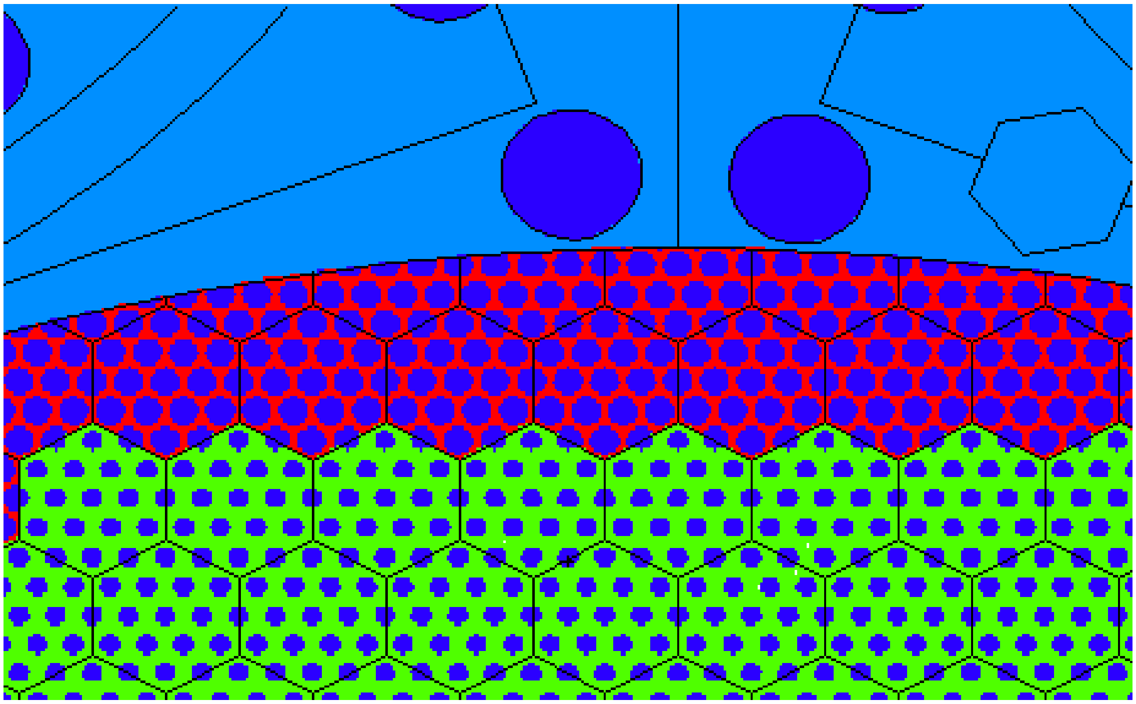
Fig. 5.1. Image of the outer periphery assemblies (red and dark blue) compared to the rest of the fuel assemblies (green and dark blue); Green- 93% enriched fuel; Red- 85% enriched fuel; Light blue- Be reflector; Dark blue- hydrogen coolant channels

The initial thought was that by drastically decreasing the amount of fissionable material through dropping the enrichment by 8% and the total volume by almost half, the power in this area would also decrease. However, this was not the case. It appeared that the increase in the amount of coolant to the area produced better moderation for the reactor essentially negating the effects that the other variables should have produced in regards to the radial power distribution (Fig. 5.2). The larger coolant channels ended up producing a slightly larger power spike than the previous design.

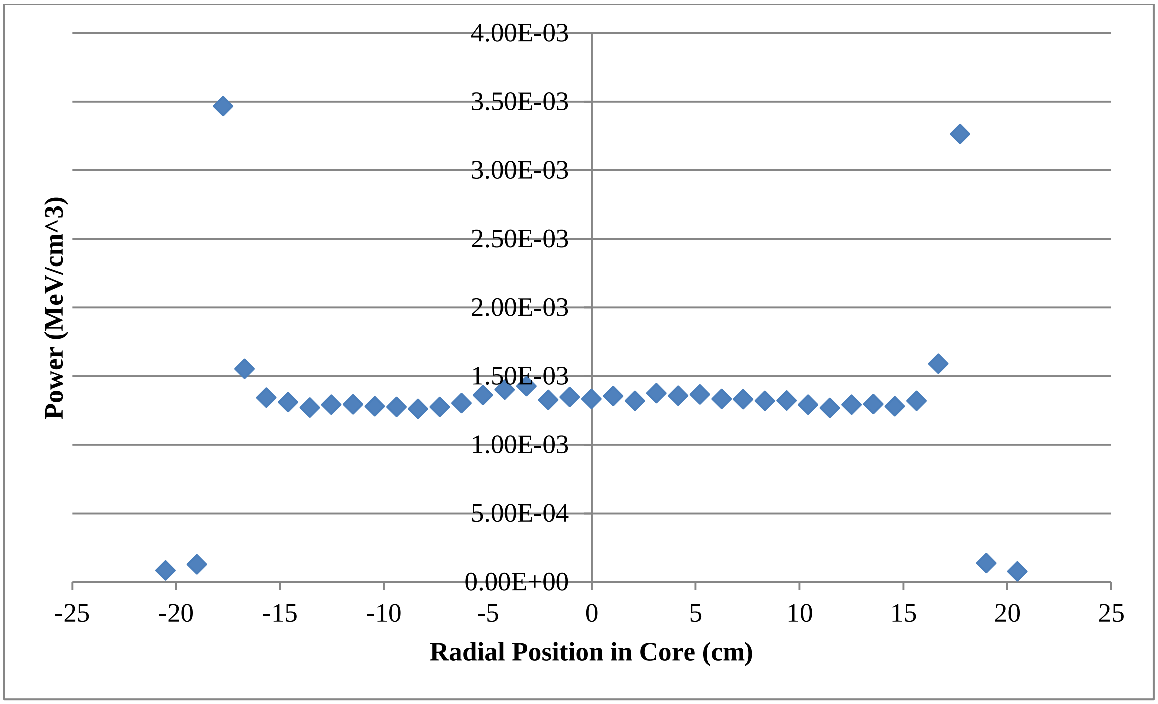

Fig. 5.2. Radial power distribution of W-Ta-UO_2 core; 18.2cm radius; CDs *out*; 6 zone radial enrichment with large 2.122mm diameter axial coolant channels around outer core periphery and 85% enriched U-235

With these results, it became apparent that another technique would have to be used in order to alleviate this intense spike in power. Figure 5.2 above shows that the outer-most two assemblies in the core show different power levels than the rest of the more central assemblies. Hereby, something had to be done in order to bring these to a baseline level. It was determined that two outer regions would have to be made in order to remedy this problem.

5.2. Final Attempt

The first step was to return the coolant channel voids around the periphery back to their original diameter of 1.5mm. The next was to slightly reduce the thickness of the outer ring of fuel assemblies and add in a secondary, one assembly thick region inside the outer ring. These modifications can be observed in Figure 5.3.

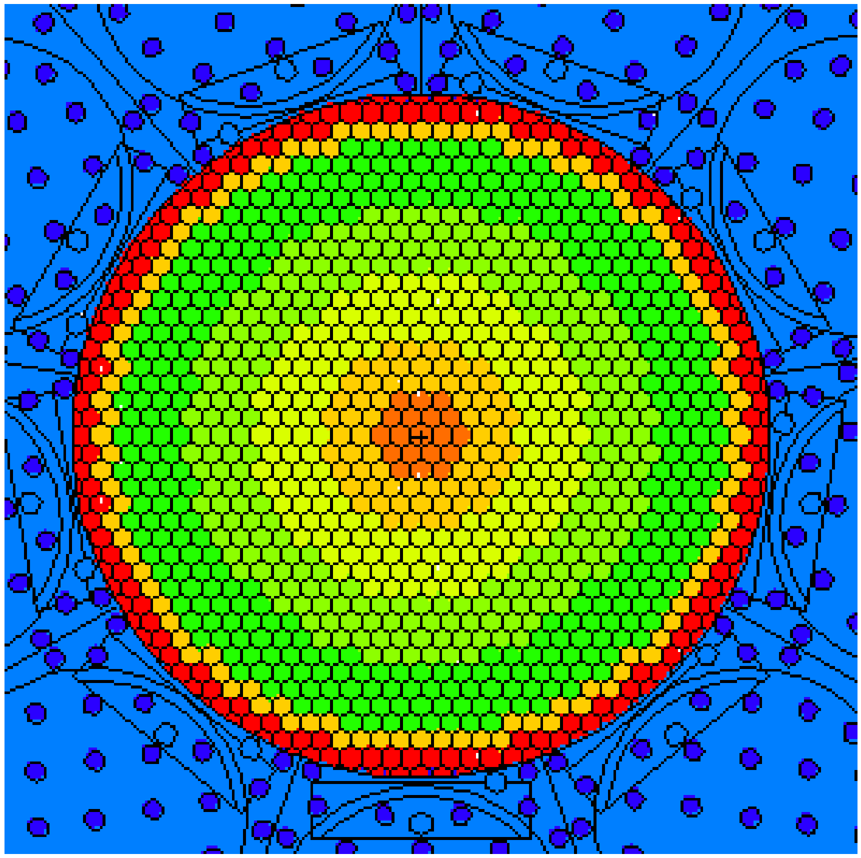

Fig. 5.3. 7 region core design; 18.2cm core; CDs out;
Outer region- 50% enriched U-235 (red);
Inside red- 87% enriched U-235 (orange);
Inner regions match original design

In the outer-most ring of assemblies, the enrichment was dropped to 50% in order to compensate for the large power spike around the outside. The next region in was only dropped from 93% down to 87% enriched U-235, because the spike in not nearly as drastic in these assemblies. The resulting power distribution proved to be vastly different near the reflector (Fig. 5.4).

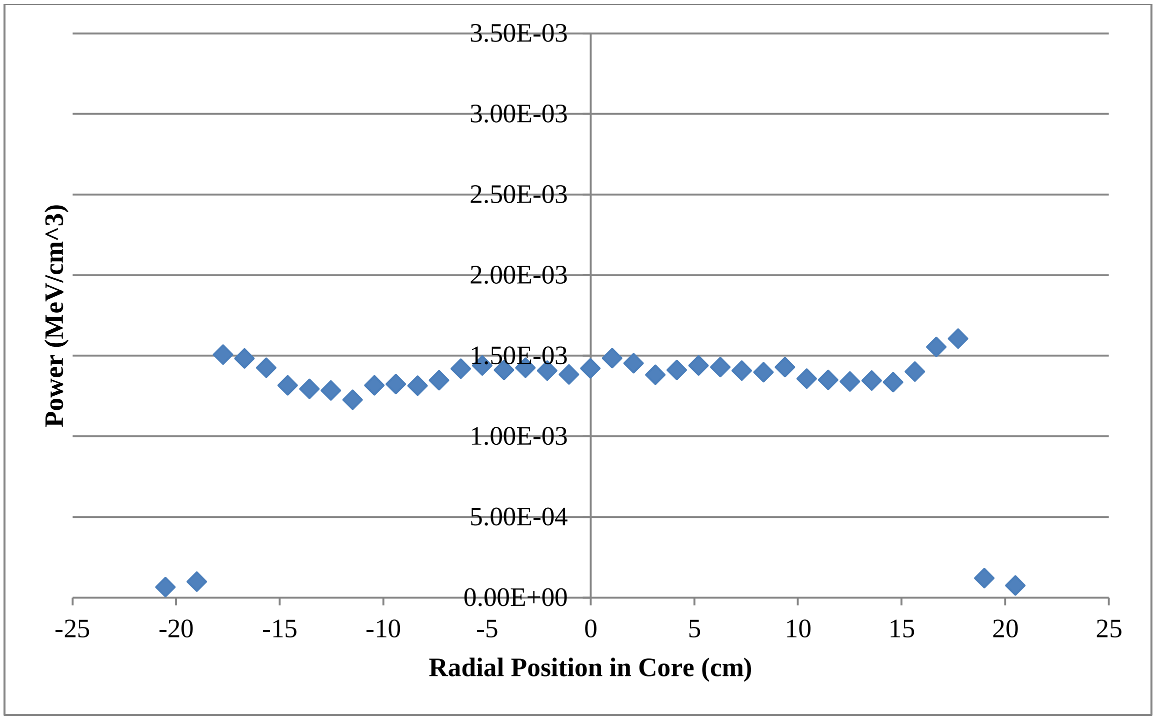

Fig. 5.4. Dampened core periphery radial power distribution of W-Ta-UO_2 core; 18.2cm radius; CDs out; 7 zone radial enrichment

The resulting power distribution displays a dampened power near the reflector. As this was the goal of manipulating the assemblies around the periphery, it was determined that the proposed geometry would be adequate to claim that the power was successfully flattened. However, it should be noted that the rest of the core displayed a slightly enhanced variation in regards to the power fluctuations between enrichment zones. This behavior was classified as approximately negligible as the power changes may be due largely to the asymmetry of the reactor.

The power distribution of a single enrichment loading can be seen in Figure 5.5. It should be noted that the power shows a peak in the middle and consistently drops and as the assemblies move further away from the center. Again, the power spike is seen near the reflector. This is the reason that the various radial enrichment zones were used to manipulate the power observed in the core to be approximately flat all the way out to the reflector.

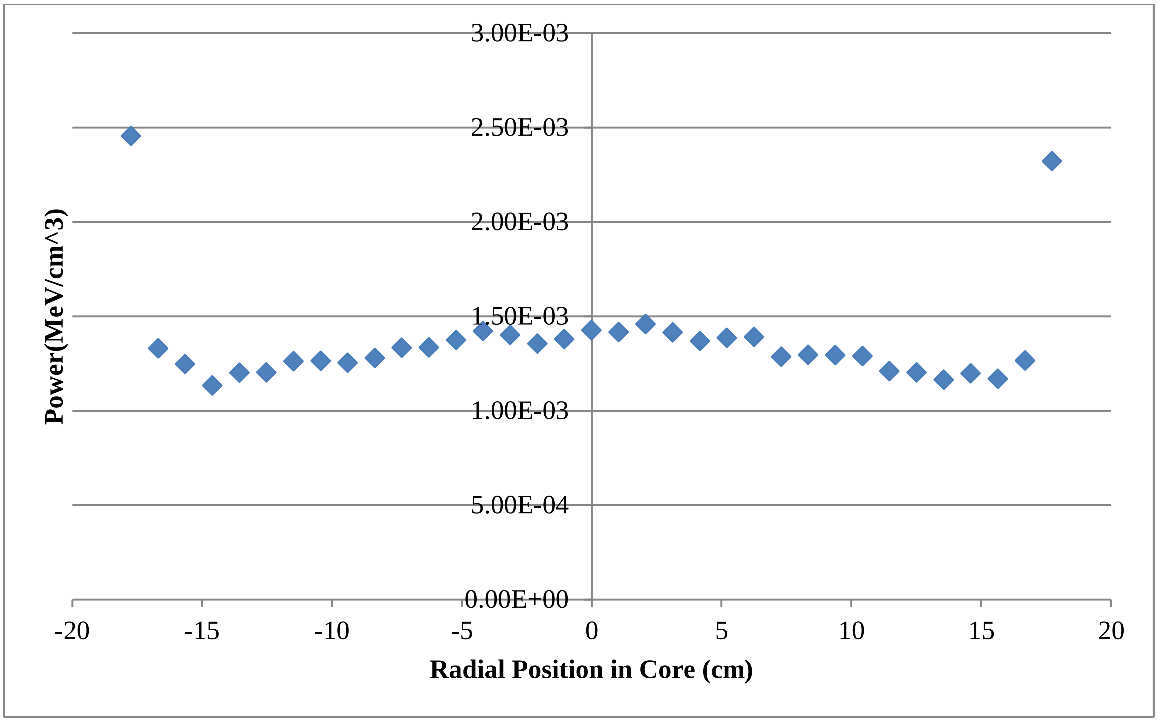

Fig. 5.5. Flat radial enrichment across the core; 9 CDs out; W-Ta-UO_2 core; 18.2cm radius

Another aspect of the process was determining the range in k_{eff} values that each configuration presents. It can be seen in the first Ta configuration listed, which is consistent with the previously designed Re configurations, that the range in k_{eff} is approximately two percent higher (Table 5.1). As mentioned previously, this is the reason for testing the core using the W-Ta-UO_2 material. The final design results are highlighted below.

The final test that was run involved the scenario of decreased or no hydrogen flow through the core. The axial channels that were previously filled with hydrogen were instead put under vacuum in order to observe the effects. The lack of moderation provides approximately a 0.6% decrease in k_{eff} which can be observed in table 5.1.

Table 5.1. k_{eff} values for various design specifications defined above

	9 CDs In:		***9 CDs Out:***		
Configuration	keff	STDEV	keff	STDEV	Δ keff
Ta 93% Single Enrmt.	NA	NA	1.08358	0.00231	NA
Re 5 Zone Enrmt.	0.93773	0.00184	1.03936	0.00212	0.10163
Ta 5 Zone Enrmt.	0.94836	0.00193	1.06869	0.00212	0.12033
Ta Lrg. Periph. Channels	NA	NA	1.03811	0.00209	NA
Ta Decrease Periph. Enrmt.	0.94849	0.00175	1.04665	0.00192	0.09816
No H Flow Through Core	NA	NA	1.04053	0.00222	NA

Although the 5-zone enrichment provides the largest range in k_{eff}, it does not provide the proper power distribution. It can be seen in Table 5.1 that the decreased periphery enrichment seen in the final 7-zone model provides an adequate 10% range in k_{eff}, along with the most flat power distribution across the entire core.

6.0. CONCLUSIONS

6.1. Mars Trajectory Mission Plan

The construction of this reactor is for the sole purpose of providing thrust for engines involved in propelling multiple rockets to Mars. The overall journey to Mars and back is broken up into multiple different missions, two of which are to be carried out a couple years prior to the actual piloted launch (Borowski, 1993). The actual dry mass of the piloted vehicle is approximately 111 tons. The purposes for these initial unpiloted missions are to send supplies into the Mars orbits.

The initial mission involves dropping 93 metric tons of liquid hydrogen (LH_2) in a storage tank into Mars orbit while awaiting the arrival of the second cargo vehicle coupled with the Earth return stage vehicle. A separate return stage vehicle and the storage tank join together in orbit to wait for the arrival of the piloted vehicle.

The piloted vehicle, assembled in Earth's orbit, later leaves headed to Mars on about a 180 day leg. The core of each NTR thruster is capable of power levels of up to 600MW thermal, which is adequate to accomplish short burns required for this trip (Fischhaber, 2012). Upon arrival at Mars, an extended period of time is spent in orbit waiting to meet up with the Earth return vehicle. From here, the crew descends to the Mars surface for an exploration, length to be determined, before returning to the fully assembled return vehicle. After a 180 day return trip, they arrive back in Earth's orbit and descend back into the atmosphere.

6.2. CONCLUSIONS: TOTAL BURN-UP AND EXCESS REACTIVITY

An important aspect of creating an effective NTR is to make sure there is enough excess reactivity (k_{excess}) to make it to Mars and back without losing power. Given the various burn times coupled with parasitic power losses, only approximately 0.3% burn-up per engine will have occurred by the end of the mission (Borowski, 1993). Being that this number is almost negligible, this number was made over a factor of 10 higher to ensure that there definitely is enough k_{excess} to ensure a successful roundtrip mission. A 5% burn-up was assumed on the final design in order to reach such conclusions. The results along with the final design specifications can be seen in Tables 6.1 and 6.2 respectively. The power distribution after 5% burn-up is displayed in Figure 6.1. Figure 5.3 displayed previously provides an image of the final design.

Table 6.1. Comparing criticality of reactor prior to launch from Earth orbit to post mission BU; CDs out

Enrichments	keff	STDEV
Initial Enrichment	1.04665	0.00192
After 5% BU	1.02446	0.00216

Table 6.2. NTR final design specifications

Design Specification	Value	Units
Core Radius	18.2	cm
Reflector Thickness	17.0	cm
Core Height	70.0	cm
B4C Thickness	6.0	mm
Radial Enrmt. Zones	7	zones

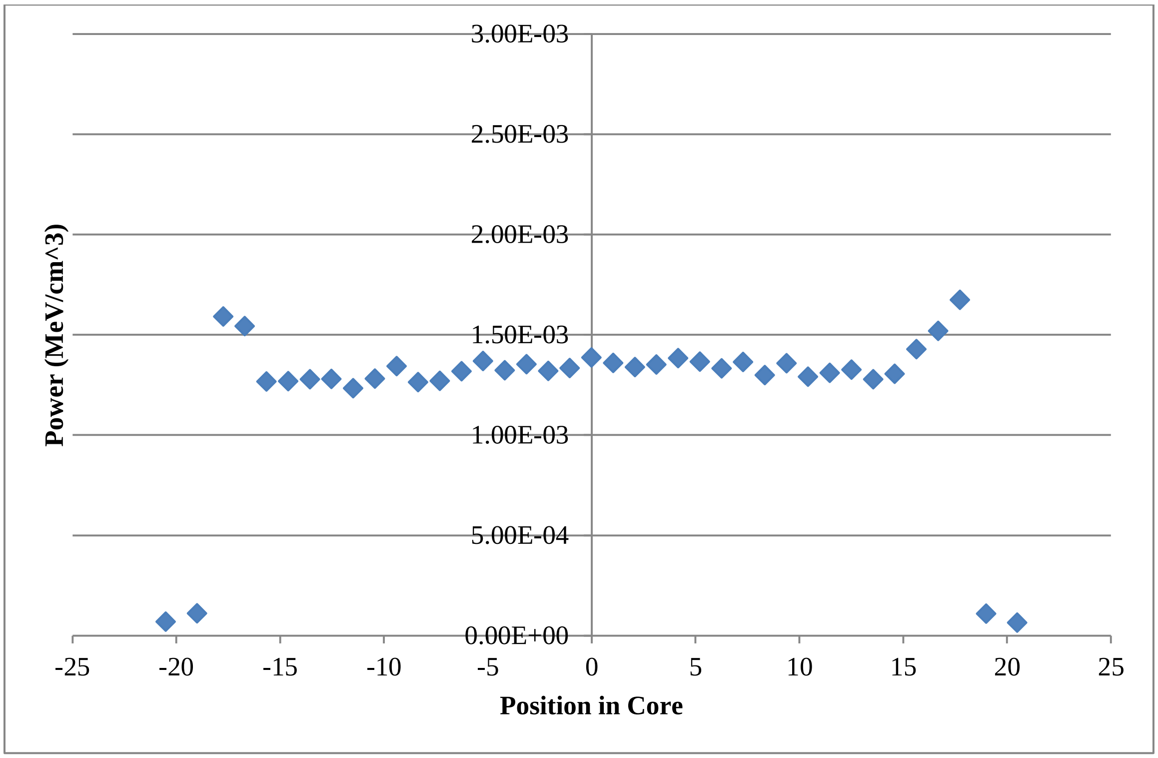

Fig. 6.1. Power distribution after 5% BU on the core; CDs out

This 5% margin is considered more than adequate to cover other aspects that may affect k_{eff}, such as fission product poisoning, temperature coefficient, and other minor factors contributing to the burn-up of U-235. Being that this is mostly a fast spectrum reactor, with minimal fissions in the Xe-135 thermal absorption cross section range, Xe-135 poisoning is essentially not an issue and each NTR engine will have no issue maintaining criticality of the core.

References

[1] Koenig, Daniel. Los Alamos National Laboratory, "Experience Gained from the Space Nuclear Rocket Program (Rover)." Los Alamos, 1986. Print.

[2] Borowski, Stanley; Corban, Robert; McGuire, Melissa; Beke, Erik. "Nuclear Thermal Rocket/Vehicle Design Options for Future NASA Missions to the Moon and Mars." NASA Technical Memo 107071. Huntsville, Alabama, Sept, 1993. <http://trajectory.grc.nasa.gov/aboutus/papers/AIAA-93-4170.pdf>

[3] "What is Specific Impulse?" Qualitative Reasoning Group. 22 December, 2009. <http://www.qrg.northwestern.edu/>.

[4] Karlheinz, Tom; Sneider, Richard T. Research on Uranium Plasmas and Their Technological Applications, Proceedings of the symposium at the University of Florida. NASA SP-236, January 1970.

[5] "Sigma Aldrich." Sigma-Aldrich Co. LLC. 201. < http://www.sigmaaldrich.com/united-states.html>.

[6] Zandbergen, B. "Thermo-Nuclear Systems." Delft University of Technology, 2013. < http://www.lr.tudelft.nl/?id=26234&L=1>.

[7] Hone, Lance; Fell, Clifford. "Nuclear Reactor for Man Mars Mission: Core Design and Fuel Materials." Senior Design Project, Idaho State University, 2013.

[8] Fischhaber, Lucas. "Next Step in the Evolution of the Nuclear Thermal Rocket." MS Thesis, Idaho State University, 2012.

[9] Schnitzler, Bruce G. "Small Reactor Designs Suitable for Direct Nuclear Thermal Propulsion: Interim Report." Space Nuclear Systems and Technologies Division, Idaho Falls, Jan, 2012. <http://www.inl.gov/technicalpublications/Documents/5394162.pdf>.

[10] Borowski, Stanley k., McCurdy, David R., Packard, Thomas W. Nuclear Thermal Propulsion (NTP): "A proven Growth Technology for Human NEO / Mars Exploration Missions." NASA, 2012. <http://www.ntrs.nasa.gov/archive/nasa/casi.ntrs.nasa.gov/20120003776_2012004085.pdf>.

7. APPENDIX A- FIGURES AND TABLES

Table 7.1. MCNP input deck isotopic abundance by weight fraction to define solid materials inside the core; W-Ta-UO_2 (89% enriched U-235 in this example); Uranium values vary based on enrichment;

Isotope	Abundance	Molar Mass	Weight % of Core	Weight Abundance	Mass (g)
Ta-181	1.0	181.0	0.25	1.0000	106379
W-182	0.265	182.0	0.75	0.262347694	96567
W-183	0.1431	183.0	0.75	0.142446149	52433
W-184	0.3076	184.0	0.75	0.307867711	113322
W-186	0.2843	186.0	0.75	0.287640339	105877
U-235	0.89	235.0	NA	0.783333333	219085
U-238	0.11	238.0	NA	0.096962963	27119
O-16	1.0	16.0	NA	0.11975697	33494
				Sum:	754275

Isotope	Density (g/cm^3)	Weight Fraction
Ta-181	16.69	0.14103
W-182		0.12803
W-183		0.06951
W-184		0.15024
W-186	19.25	0.14037
U-235		0.29046
U-238		0.03595
O-16	10.97	0.04441
	14.79	1.00000

Volume Fraction Fuel:	0.7
Volume Fraction (UO2):	0.5
Radius of Core (cm):	18.2
Height of Core (cm):	70.0
Volume of Core (cm^3):	72843.5

Table 7.2. MCNP input deck isotopic abundance by weight fraction to define solid materials inside the core; W-Re-UO_2 (89% enriched U-235 in this example); Uranium values vary based on enrichment;

Isotope	Abundance	Molar Mass	Weight % of Core	Weight Abundance	Mass (g)
Re-185	0.374	185.0	0.25	0.371569733	49782
Re-187	0.626	187.0	0.25	0.628655819	84226
W-182	0.265	182.0	0.75	0.262347694	96567
W-183	0.1431	183.0	0.75	0.142446149	52433
W-184	0.3076	184.0	0.75	0.307867711	113322
W-186	0.2843	186.0	0.75	0.287640339	105877
U-235	0.89	235.0	NA	0.783333333	219085
U-238	0.11	238.0	NA	0.096962963	27119
O-16	1.0	16.0	NA	0.11975697	33494
				Sum:	781903

Isotope	Density (g/cm^3)	Weight Fraction
Re-185		0.06367
Re-187	21.02	0.10772
W-182		0.12350
W-183		0.06706
W-184		0.14493
W-186	19.25	0.13541
U-235		0.28019
U-238		0.03468
O-16	10.97	0.04284
	15.33125	1.00000

Volume Fraction Fuel:	0.7
Volume Fraction (UO2):	0.5
Radius of Core (cm):	18.2
Height of Core (cm):	70.0
Volume of Core (cm^3):	72843.5

8. APPENDIX B- MCNP INPUT DECK

```
C Cell Cards
4 0 -40 fill=20 imp:n=1 $ Fill assemblies into core
5 0 -20 lat=2 u=20 fill=-21:21 -21:21 0:0 &
2 2 2 2 2 2 2 2 2 2 2 2 2 2 2 2 2 2 2 2 2 2 2 2 2 2 &
2 2 2 2 2 2 2 2 2 2 2 2 2 2 2 2 2 &
2 2 2 2 2 2 2 2 2 2 4 4 4 4 4 4 4 4 4 4 4 4 4 4 4 4 &
4 4 4 4 4 4 4 4 4 4 4 4 4 4 4 4 4 &
4 4 4 4 4 4 4 4 4 4 4 4 4 4 4 4 4 4 4 4 4 4 4 4 4 4 &
4 4 4 4 4 4 4 4 4 4 4 4 4 4 4 4 4 &
2 2 2 2 2 2 2 2 2 2 2 2 2 2 2 2 2 2 2 2 4 4 4 4 4 4 &
6 6 6 6 6 6 6 6 6 4 4 4 4 2 2 2 2 &
2 2 2 2 2 2 2 2 2 2 2 2 2 2 2 2 2 2 2 4 4 4 4 6 6 6 &
2 2 2 2 2 2 2 2 6 6 6 4 4 4 2 2 2 &
2 2 2 2 2 2 2 2 2 2 2 2 2 2 2 2 2 2 4 4 4 6 6 2 2 2 &
2 2 2 2 2 2 2 2 2 2 6 6 4 4 4 2 2 &
2 2 2 2 2 2 2 2 2 2 2 2 2 2 2 2 4 4 4 6 6 2 2 2 2 2 &
2 2 2 2 2 2 2 2 2 2 2 6 6 4 4 4 2 &
2 2 2 2 2 2 2 2 2 2 2 2 2 2 4 4 4 4 6 2 2 2 2 2 2 2 &
2 2 2 2 2 2 2 2 2 2 2 2 6 4 4 4 4 &
2 2 2 2 2 2 2 2 2 2 2 2 2 4 4 4 6 6 2 2 2 2 2 2 2 1 &
1 1 1 1 1 2 2 2 2 2 2 2 6 6 4 4 4 &
2 2 2 2 2 2 2 2 2 2 2 2 4 4 4 6 2 2 2 2 2 2 1 1 1 1 &
1 1 1 1 1 1 1 2 2 2 2 2 2 6 4 4 4 &
2 2 2 2 2 2 2 2 2 2 2 4 4 4 6 2 2 2 2 2 2 1 1 1 1 1 &
1 1 1 1 1 1 1 2 2 2 2 2 2 6 4 4 4 &
2 2 2 2 2 2 2 2 2 2 4 4 4 6 2 2 2 2 2 1 1 1 1 1 1 1 &
1 1 1 1 1 1 1 1 2 2 2 2 2 6 4 4 4 &
2 2 2 2 2 2 2 2 2 4 4 4 6 2 2 2 2 2 1 1 1 1 1 9 9 9 &
9 9 9 1 1 1 1 1 2 2 2 2 2 6 4 4 4 &
2 2 2 2 2 2 2 2 4 4 4 6 2 2 2 2 1 1 1 1 1 9 9 9 9 9 &
9 9 9 9 1 1 1 1 1 2 2 2 2 6 4 4 4 &
2 2 2 2 2 2 2 4 4 4 6 2 2 2 2 1 1 1 1 1 9 9 9 9 9 9 &
9 9 9 9 1 1 1 1 1 2 2 2 2 6 4 4 4 &
2 2 2 2 2 2 4 4 4 6 2 2 2 2 1 1 1 1 9 9 9 9 9 9 9 9 &
9 9 9 9 9 1 1 1 1 2 2 2 2 6 4 4 4 &
2 2 2 2 2 2 4 4 6 2 2 2 2 1 1 1 1 9 9 9 9 9 6 6 6 6 &
9 9 9 9 9 1 1 1 1 2 2 2 2 6 4 4 2 &
2 2 2 2 2 4 4 4 6 2 2 2 1 1 1 1 9 9 9 9 6 6 6 6 6 6 &
6 9 9 9 9 1 1 1 1 2 2 2 6 4 4 4 2 &
2 2 2 2 4 4 4 6 2 2 2 2 1 1 1 9 9 9 9 6 6 6 6 6 6 6 &
6 9 9 9 9 1 1 1 2 2 2 2 6 4 4 4 2 &
2 2 2 2 4 4 6 2 2 2 2 1 1 1 9 9 9 9 6 6 6 3 3 3 6 6 &
6 9 9 9 9 1 1 1 2 2 2 2 6 4 4 2 2 &
2 2 2 4 4 4 6 2 2 2 1 1 1 1 9 9 9 6 6 6 3 3 3 3 6 6 &
```

6 9 9 9 1 1 1 1 2 2 2 6 4 4 4 2 2 &
2 2 2 4 4 6 2 2 2 2 1 1 1 9 9 9 9 6 6 3 3 3 3 3 6 6 &
9 9 9 9 1 1 1 2 2 2 2 6 4 4 2 2 2 & $ Middle
2 2 4 4 4 6 2 2 2 1 1 1 1 9 9 9 6 6 6 3 3 3 3 6 6 6 &
9 9 9 1 1 1 1 2 2 2 6 4 4 4 2 2 2 &
2 2 4 4 6 2 2 2 2 1 1 1 9 9 9 9 6 6 6 3 3 3 6 6 6 9 &
9 9 9 1 1 1 2 2 2 2 6 4 4 2 2 2 2 &
2 4 4 4 6 2 2 2 2 1 1 1 9 9 9 9 6 6 6 6 6 6 6 6 9 9 &
9 9 1 1 1 2 2 2 2 6 4 4 4 2 2 2 2 &
2 4 4 4 6 2 2 2 1 1 1 1 9 9 9 9 6 6 6 6 6 6 6 9 9 9 &
9 1 1 1 1 2 2 2 6 4 4 4 2 2 2 2 2 &
2 4 4 6 2 2 2 2 1 1 1 1 9 9 9 9 9 6 6 6 6 9 9 9 9 9 &
1 1 1 1 2 2 2 2 6 4 4 2 2 2 2 2 2 &
4 4 4 6 2 2 2 2 1 1 1 1 9 9 9 9 9 9 9 9 9 9 9 9 9 1 &
1 1 1 2 2 2 2 6 4 4 4 2 2 2 2 2 2 &
4 4 4 6 2 2 2 2 1 1 1 1 1 9 9 9 9 9 9 9 9 9 9 1 1 1 &
1 1 2 2 2 2 6 4 4 4 2 2 2 2 2 2 2 &
4 4 4 6 2 2 2 2 1 1 1 1 1 9 9 9 9 9 9 9 9 9 1 1 1 1 &
1 2 2 2 2 6 4 4 4 2 2 2 2 2 2 2 2 &
4 4 4 6 2 2 2 2 2 1 1 1 1 1 9 9 9 9 9 9 1 1 1 1 1 2 &
2 2 2 2 6 4 4 4 2 2 2 2 2 2 2 2 2 &
4 4 4 6 2 2 2 2 2 1 1 1 1 1 1 1 1 1 1 1 1 1 1 1 2 2 &
2 2 2 6 4 4 4 2 2 2 2 2 2 2 2 2 2 &
4 4 4 6 2 2 2 2 2 1 1 1 1 1 1 1 1 1 1 1 1 1 1 2 2 2 &
2 2 6 4 4 4 2 2 2 2 2 2 2 2 2 2 2 &
4 4 4 6 2 2 2 2 2 2 1 1 1 1 1 1 1 1 1 1 1 2 2 2 2 2 &
2 6 4 4 4 2 2 2 2 2 2 2 2 2 2 2 2 &
4 4 4 6 6 2 2 2 2 2 2 2 1 1 1 1 1 1 2 2 2 2 2 2 2 6 &
6 4 4 4 2 2 2 2 2 2 2 2 2 2 2 2 2 &
2 4 4 4 6 2 2 2 2 2 2 2 2 2 2 2 2 2 2 2 2 2 2 2 6 4 &
4 4 2 2 2 2 2 2 2 2 2 2 2 2 2 2 2 &
2 4 4 4 6 6 2 2 2 2 2 2 2 2 2 2 2 2 2 2 2 2 6 6 4 4 &
2 2 2 2 2 2 2 2 2 2 2 2 2 2 2 2 2 &
2 2 4 4 4 6 6 2 2 2 2 2 2 2 2 2 2 2 2 2 6 6 4 4 4 2 &
2 2 2 2 2 2 2 2 2 2 2 2 2 2 2 2 2 &
2 2 2 4 4 4 6 6 6 2 2 2 2 2 2 2 6 6 6 4 4 4 2 2 2 &
2 2 2 2 2 2 2 2 2 2 2 2 2 2 2 2 2 &
2 2 2 2 4 4 4 4 6 6 6 6 6 6 6 6 6 4 4 4 4 2 2 2 2 2 &
2 2 2 2 2 2 2 2 2 2 2 2 2 2 2 2 2 &
4 4 4 4 4 4 4 4 4 4 4 4 4 4 4 4 4 4 4 4 4 4 4 4 2 2 &
2 2 2 2 2 2 2 2 2 2 2 2 2 2 2 2 2 &
2 2 2 2 2 2 2 4 4 4 4 4 4 4 4 4 4 2 2 2 2 2 2 2 2 2 &
2 2 2 2 2 2 2 2 2 2 2 2 2 2 2 2 2 &
2 2 2 2 2 2 2 2 2 2 2 2 2 2 2 2 2 2 2 2 2 2 2 2 2 2 &
2 2 2 2 2 2 2 2 2 2 2 2 2 2 2 2 2 &
imp:n=1$ Fully specified fill of core

```
6 0 -21 fill=19 u=2 imp:n=1 $ Place units into assemblies
7 0 -18 fill=18 u=19 lat=2 imp:n=1 $ Hex .7 Fuel, .3 H
8 10 -14.79 17 u=18 imp:n=1 $ Fuel
9 6 -0.000089 -17 u=18 imp:n=1 $ Core H coolant channels
11 0 -21 fill=17 u=1 imp:n=1 $ Place units into assemblies
12 0 -18 fill=16 u=17 lat=2 imp:n=1 $ Hex .7 Fuel, .3 H
13 11 -14.79 17 u=16 imp:n=1 $ Fuel
14 6 -0.000089 -17 u=16 imp:n=1 $ Core H coolant channels
16 0 -21 fill=15 u=9 imp:n=1 $ Place units into assemblies
17 0 -18 fill=14 u=15 lat=2 imp:n=1 $ Hex .7 Fuel, .3 H
18 12 -14.79 17 u=14 imp:n=1 $ Fuel
19 6 -0.000089 -17 u=14 imp:n=1 $ Core H coolant channels
21 0 -21 fill=13 u=6 imp:n=1 $ Place units into assemblies
22 0 -18 fill=12 u=13 lat=2 imp:n=1 $ Hex .7 Fuel, .3 H
23 13 -14.79 17 u=12 imp:n=1 $ Fuel
24 6 -0.000089 -17 u=12 imp:n=1 $ Core H coolant channels
27 0 -21 fill=11 u=3 imp:n=1 $ Place units into assemblies
28 0 -18 fill=10 u=11 lat=2 imp:n=1 $ Hex .7 Fuel, .3 H
29 14 -14.79 17 u=10 imp:n=1 $ Fuel
30 6 -0.000089 -17 u=10 imp:n=1 $ Core H coolant channels
31 0 -21 fill=23 u=4 imp:n=1 $ Place units into assemblies
32 0 -18 fill=22 u=23 lat=2 imp:n=1 $ Hex .4 Fuel, .6 H
33 15 -14.79 17 u=22 imp:n=1 $ Outer fuel region w/ large coolant channels
34 6 -0.000089 -17 u=22 imp:n=1 $ Large core coolant channels
C cells 36-39 define drums with B4C rotated out
36 7 -1.85 -53 -55 #79 #81 u=30 imp:n=1 $ Fill inside box and in drum with Be
37 7 -1.85 -55 52 #72 #73 u=30 imp:n=1 $ Fill outside drum and in box with Be
38 8 -2.52 -52 -55 53 u=30 imp:n=1 $ B4C section (comment out)
c 39 7 -1.85 -52 -55 53 u=30 imp:n=1 $ B4C replace with Be (comment out)
C Fill outside drum and H coolant with Be
40 7 -1.85 31 52 54 55 60 #71 #72 #73 #74 #75 #76 #77 #83 #84 #85 #90 #100 &
#104 #105 #108 #109 #110 u=30 imp:n=1 $ Fill outside drum and box with Be
41 7 -1.85 -52 54 55 #78 #80 #82 #86 #87 #88 #89 #91 #92 #93 #94 #95 #96 #97 &
#98 #99 #101 #102 #103 u=30 imp:n=1 $ Fill inside drum outside box with Be
C cells 42-45 define drums with B4C rotated in
42 7 -1.85 30 -53 -54 #106 #107 u=30 imp:n=1 $ Fill inside box and in drum with Be
43 7 -1.85 31 -54 52 #105 #108 u=30 imp:n=1 $ Fill outside drum and in box with Be
c 44 8 -2.52 -52 -54 53 u=30 imp:n=1 $ B4C section (comment out)
45 7 -1.85 -52 -54 53 u=30 imp:n=1 $ B4C replace with Be (comment out)
C The next 18 lines rotate the single control drum section 9 times around the core
47 0 40 -50 fill=40 imp:n=1
48 0 -4 -5 fill=30 u=40 imp:n=1
49 0 4 -7 fill=51 u=40 imp:n=1
50 0 -2:2 fill=30 trcl=1 u=51 imp:n=1
51 0 7 -8 fill=52 u=40 imp:n=1
52 0 -2:2 fill=30 trcl=2 u=52 imp:n=1
```

```
53 0 8 -10 fill=53 u=40 imp:n=1
54 0 -2:2 fill=30 trcl=3 u=53 imp:n=1
55 0 10 12 fill=54 u=40 imp:n=1
56 0 -2:2 fill=30 trcl=4 u=54 imp:n=1
57 0 -12 11 fill=55 u=40 imp:n=1
58 0 -2:2 fill=30 trcl=5 u=55 imp:n=1
59 0 -11 9 fill=56 u=40 imp:n=1
60 0 -2:2 fill=30 trcl=6 u=56 imp:n=1
61 0 -9 6 fill=57 u=40 imp:n=1
62 0 -2:2 fill=30 trcl=7 u=57 imp:n=1
63 0 -6 5 fill=58 u=40 imp:n=1
64 0 -2:2 fill=30 trcl=8 u=58 imp:n=1
C Cells 70-110 define the hydrogen channels through the reflector
70 6 -0.000089 -60 u=30 imp:n=1
71 like 70 but trcl (2.6 -0.8 0) u=30 imp:n=1
72 like 70 but trcl (5.3 -1.3 0) u=30 imp:n=1
73 like 70 but trcl (16.6 -1.3 0) u=30 imp:n=1
74 like 70 but trcl (19.3 -0.8 0) u=30 imp:n=1
75 like 70 but trcl (21.8 0.0 0) u=30 imp:n=1 $ End row 1
76 like 70 but trcl (0.9 2.2 0) u=30 imp:n=1
77 like 70 but trcl (3.4 1.5 0) u=30 imp:n=1
78 like 70 but trcl (7.0 1.3 0) u=30 imp:n=1
79 like 70 but trcl (9.0 -0.5 0) u=30 imp:n=1
80 like 70 but trcl (11.0 1.3 0) u=30 imp:n=1
81 like 70 but trcl (13.0 -0.5 0) u=30 imp:n=1
82 like 70 but trcl (15.0 1.3 0) u=30 imp:n=1
83 like 70 but trcl (18.6 1.5 0) u=30 imp:n=1
84 like 70 but trcl (21.1 2.2 0) u=30 imp:n=1 $ End row 2
85 like 70 but trcl (1.7 4.4 0) u=30 imp:n=1
86 like 70 but trcl (5.0 3.6 0) u=30 imp:n=1
87 like 70 but trcl (9.0 3.6 0) u=30 imp:n=1
88 like 70 but trcl (13.0 3.6 0) u=30 imp:n=1
89 like 70 but trcl (17.0 3.6 0) u=30 imp:n=1
90 like 70 but trcl (20.3 4.4 0) u=30 imp:n=1 $ End row 3
91 like 70 but trcl (4.0 5.8 0) u=30 imp:n=1
92 like 70 but trcl (7.0 5.8 0) u=30 imp:n=1
93 like 70 but trcl (11.0 5.8 0) u=30 imp:n=1
94 like 70 but trcl (15.0 5.8 0) u=30 imp:n=1
95 like 70 but trcl (18.0 5.8 0) u=30 imp:n=1 $ End row 4
96 like 70 but trcl (5.0 8.2 0) u=30 imp:n=1
97 like 70 but trcl (9.0 8.2 0) u=30 imp:n=1
98 like 70 but trcl (13.0 8.2 0) u=30 imp:n=1
99 like 70 but trcl (17.0 8.2 0) u=30 imp:n=1 $ End row 5
100 like 70 but trcl (3.9 11.0 0) u=30 imp:n=1
101 like 70 but trcl (7.0 10.4 0) u=30 imp:n=1
102 like 70 but trcl (11.0 10.4 0) u=30 imp:n=1
```

```
103 like 70 but trcl (15.0 10.4 0) u=30 imp:n=1
104 like 70 but trcl (18.1 11.0 0) u=30 imp:n=1 $ End row 6
105 like 70 but trcl (5.5 12.6 0) u=30 imp:n=1
106 like 70 but trcl (9.0 12.2 0) u=30 imp:n=1
107 like 70 but trcl (13.0 12.2 0) u=30 imp:n=1
108 like 70 but trcl (16.5 12.6 0) u=30 imp:n=1 $ End row 7
109 like 70 but trcl (5.2 14.5 0) u=30 imp:n=1
110 like 70 but trcl (16.5 14.5 0) u=30 imp:n=1
200 7 -1.85 -31 u=30 imp:n=1 $ Refl power distribution assembly
201 7 -1.85 -30 u=30 imp:n=1 $ Refl power distribution assembly
999 0 50 -999 imp:n=0

C Surface Cards
2 pz -35.0
4 p 0 0 0 -0.34202 0.93969 0 -0.34202 0.93969 1.0 $ 20 degrees
5 p 0 0 0 0.34202 0.93969 0 0.34202 0.93969 1.0 $ 340 degrees
6 p 0 0 0 0.86602 0.5 0 0.86602 0.5 1.0 $ 300 deg
7 p 0 0 0 0.86602 -0.5 0 0.86602 -0.5 1.0 $ 60 deg
8 p 0 0 0 -0.98481 -0.17365 0 -0.98481 -0.17365 1.0 $ 100 deg
9 p 0 0 0 0.98481 -0.17365 0 0.98481 -0.17365 1.0 $ 260 deg
10 p 0 0 0 -0.64279 -0.76604 0 -0.64279 -0.76604 1.0 $ 140 deg
11 p 0 0 0 0.64279 -0.76604 0 0.64279 -0.76604 1.0 $ 220 deg
12 p 0 0 0 0 -1.0 0 0 -1.0 1.0 $ 180 deg
16 rcc 0 0 -35 0 0 70 0.1061 $ Outer periphery coolant channels
17 rcc 0 0 -35 0 0 70 0.075 $ 1.5mm diam. H coolant channels
18 rhp 0 0 -35 0 0 70 0.1304 $ Surrounding Hex, 0.7 Fuel, 0.3 He
20 rhp 0 0 -35 0 0 70 0.5216 $ Hexagonal fuel assembly
21 rhp 0 0 -35 0 0 70 0.53 $ Slightly larger
30 rhp 0 -20.7 -35 0 0 70 0.5216 $ Be assembly for power distribution
31 rhp 3.9 -18.5 -35 0 0 70 0.5216 $ Be assembly for power distribution
40 rcc 0 0 -35 0 0 70 18.2 $ Core boundary
50 rcc 0 0 -35 0 0 70 35.2 $ 17cm Be reflector
52 rcc 0 -26.6 -35 0 0 70 8.0 $ Control Drum
53 rcc 0 -26.6 -35 0 0 70 7.4 $ B4C Section ring
54 rpp -5.65685 5.65685 -21.4 -18.5 -35 35 $ Box used B4C drums in
55 rpp -5.65685 5.65685 -34.7 -31.7 -35 35 $ Box for drums out
60 rcc -10.9 -32.4 -35 0 0 70 0.5 $ Original reflector coolant channel
999 rpp -1000 1000 -1000 1000 -1000 1000 $ Box that contains our problem

C Material Cards
m1 8016 -.04284 92235 -.2928 92238 -.02207 74182 -.1235 74183 -.06706 &
74184 -.1449 74186 -.1354 75185 -.06367 75187 -.1077 $ (93% Enriched)
m2 8016 -.04284 92235 -.2865 92238 -.02838 74182 -.1235 74183 -.06706 &
74184 -.1449 74186 -.1354 75185 -.06367 75187 -.1077
C 0.50 UO2 and 0.375 W and 0.125 Re (91% Enriched)
m3 8016 -.04284 92235 -.2802 92238 -.03468 74182 -.1235 74183 -.06706 &
```

```
74184 -.1449 74186 -.1354 75185 -.06367 75187 -.1077 $ (89% Enriched)
m4 8016 -.04284 92235 -.2739 92238 -.04099 74182 -.1235 74183 -.06706 &
74184 -.1449 74186 -.1354 75185 -.06367 75187 -.1077 $ (87% Enriched)
m5 8016 -.04284 92235 -.2676 92238 -.04729 74182 -.1235 74183 -.06706 &
74184 -.1449 74186 -.1354 75185 -.06367 75187 -.1077 $ (85% Enriched)
m6 1002 -1 $ Hydrogen
m7 4009 -1 $ Beryllium
m8 5010 0.1592 5011 0.6408 6000 0.2 $ B4C
m10 8016 -.04441 92235 -.2883 92238 -.02288 74182 -.1280 74183 -.06952 &
74184 -.1502 74186 -.1404 73181 -0.1410 $ (93% Enriched)
m11 8016 -.04441 92235 -.2821 92238 -.02942 74182 -.1235 74183 -.06706 &
74184 -.1449 74186 -.1354 73181 -0.1714
C 0.50 UO2 and 0.375 W and 0.125 Ta (91% Enriched)
m12 8016 -.04441 92235 -.2759 92238 -.03595 74182 -.1235 74183 -.06706 &
74184 -.1449 74186 -.1354 73181 -0.1714 $ (89% Enriched)
m13 8016 -.04441 92235 -.2697 92238 -.04249 74182 -.1235 74183 -.06706 &
74184 -.1449 74186 -.1354 73181 -0.1714 $ (87% Enriched)
m14 8016 -.04440 92235 -0.2635 92238 -.04903 74182 -.1235 74183 -.06706 &
74184 -.1449 74186 -.1354 73181 -0.1714 $ (85% Enriched)
m15 8016 -0.4440 92235 -0.1550 92238 -0.16339 74182 -.1235 74183 -.06706 &
74184 -.1449 74186 -.1354 73181 -0.1714 $ (50% Enriched)
*tr1 0 0 0 40 50 90 130 40 90 90 90 0 $ 40 deg translation
*tr2 0 0 0 80 10 90 170 80 90 90 90 0 $ 80 deg trans
*tr3 0 0 0 120 30 90 210 120 90 90 90 0 $ 120 deg trans
*tr4 0 0 0 160 70 90 250 160 90 90 90 0 $ 160 deg trans
*tr5 0 0 0 200 110 90 290 200 90 90 90 0 $ 200 deg trans
*tr6 0 0 0 240 150 90 330 240 90 90 90 0 $ 240 deg trans
*tr7 0 0 0 280 190 90 370 280 90 90 90 0 $ 280 deg trans
*tr8 0 0 0 320 230 90 410 320 90 90 90 0 $ 320 deg trans
C Source Card
kcode 1000 1.0 25 125
ksrc 0 0 0
*FMESH4:n geom=xyz origin=-35 -1 -35 &
imesh 35 iints 280 jmesh 35 jints 280 kmesh 35 kints 1
F6:n,p (29<28<27<5[0 0 0]<4) (29<28<27<5[1 0 0]<4) (29<28<27<5[-1 0 0]<4) &
(29<28<27<5[2 0 0]<4) (29<28<27<5[-2 0 0]<4) (23<22<21<5[3 0 0]<4) &
(23<22<21<5[-3 0 0]<4) (23<22<21<5[4 0 0]<4) (23<22<21<5[-4 0 0]<4) &
(18<17<16<5[5 0 0]<4) (18<17<16<5[-5 0 0]<4) (18<17<16<5[6 0 0]<4) &
(18<17<16<5[-6 0 0]<4) (18<17<16<5[7 0 0]<4) (18<17<16<5[-7 0 0]<4) &
(18<17<16<5[8 0 0]<4) (18<17<16<5[-8 0 0]<4) (13<12<11<5[9 0 0]<4) &
(13<12<11<5[-9 0 0]<4) (13<12<11<5[10 0 0]<4) (13<12<11<5[-10 0 0]<4) &
(13<12<11<5[11 0 0]<4) (13<12<11<5[-11 0 0]<4) (8<7<6<5[12 0 0]<4) &
(8<7<6<5[-12 0 0]<4) (8<7<6<5[13 0 0]<4) (8<7<6<5[-13 0 0]<4) &
(8<7<6<5[14 0 0]<4) (8<7<6<5[-14 0 0]<4) (8<7<6<5[15 0 0]<4) &
(8<7<6<5[-15 0 0]<4) (23<22<21<5[16 0 0]<4) (23<22<21<5[-16 0 0]<4) &
```

```
(33<32<31<5[17 0 0]<4) (33<32<31<5[-17 0 0]<4) (200<52<51<47) (200<62<61<47)
        &
(201<52<51<47) (201<62<61<47)
sd6 683.0111 683.0111 683.0111 683.0111 683.0111 683.0111 683.0111 683.0111 &
683.0111 683.0111 683.0111 683.0111 683.0111 683.0111 683.0111 683.0111 &
683.0111 683.0111 683.0111 683.0111 683.0111 683.0111 683.0111 683.0111 &
683.0111 683.0111 683.0111 683.0111 683.0111 683.0111 683.0111 683.0111 &
683.0111 683.0111 683.0111 85.4341 85.4341 85.4341 85.4341
mode n
prdmp 0 0 1 0 0
print
```